

Multimedia Contents



Biomimetic

23. Biomimetic Robots

Kyu-Jin Cho, Robert Wood

Biomimetic robot designs attempt to translate biological principles into engineered systems, replacing more classical engineering solutions in order to achieve a function observed in the natural system. This chapter will focus on mechanism design for bio-inspired robots that replicate key principles from nature with novel engineering solutions. The challenges of biomimetic design include developing a deep understanding of the relevant natural system and translating this understanding into engineering design rules. This often entails the development of novel fabrication and actuation to realize the biomimetic design.

This chapter consists of four sections. In Sect. 23.1, we will define what biomimetic design entails, and contrast biomimetic robots with bio-inspired robots. In Sect. 23.2, we will discuss the fundamental components for developing a biomimetic robot. In Sect. 23.3, we will review detailed biomimetic designs that have been developed for canonical robot locomotion behaviors including flapping-wing flight, jumping, crawling, wall climbing, and swimming. In Sect. 23.4, we will discuss the enabling technologies for

23.1	Overview	544
23.2	Components of Biomimetic Robot Design	544
23.3	Mechanisms	545
23.3.1	Legged Crawling	545
23.3.2	Worm-Like Crawling	547
23.3.3	Snake Robots	548
23.3.4	Flapping-Wing Flight.....	550
23.3.5	Wall Climbing.....	551
23.3.6	Swimming	553
23.3.7	Jumping.....	555
23.3.8	Gripping and Perching.....	558
23.4	Material and Fabrication	561
23.4.1	Shape Deposition Manufacturing	561
23.4.2	Smart Composite Microstructures	562
23.4.3	Pop-Up Book MEMS	564
23.4.4	Other Fabrication Methods	565
23.5	Conclusion	567
	Video-References	568
	References	570

these biomimetic designs including material and fabrication.

Biomimetics is a broad field that covers all ranges of robotics including robot structure and mechanics, actuation, perception, and autonomy. This section will focus on robots that mimic structure and movement principles found in nature to perform desired tasks in unstructured environments.

Nature frequently inspires engineers to adopt solutions from biology for application to human challenges. Robots are built to perform certain tasks, and many tasks include moving from one place to another. The various

modes of locomotion in nature have inspired robots to mimic these locomotion with a goal to overcome various obstacles in the environment, and move around with the extreme agility similar to that found in nature. Mankind has engineered various modes of transportation on ground, air, and water. On ground, wheeled vehicles are the most popular choice. In air, fixed wing airplanes and helicopters with rotating blades dominate, and in water, ships, and submarines propelled by similar rotating elements are most common. In contrast, nature

has different solutions to locomotion involving moving legs, undulating fins, and flapping wings. Many of these biological locomotion mechanisms have analogies to engineered systems. Instead of using wheels, nature uses legs of different sizes, numbers, and impedances; humans and birds are bipedal, many mammals and reptiles move on four legs, and insects have six legs, and other arthropods have eight or more legs. These legs are coordinated to move on different surfaces in a stable manner. Snakes and worms move around without legs

by creating waves with their body. Instead of fixed wings with jets and rotary propellers, birds, bats, and flying insects flap their wings. Fish create undulatory motions with their bodies to swim with agility far beyond conventional boats and submarines. Each of these biological locomotion modes are based on the nature's fundamental actuator: muscle. Muscles create linear motion that is coupled to the structures that generate locomotion. Therefore, these structures are closely related to the morphology of the muscles that move the structures.

23.1 Overview

The main purpose of locomotion in manmade machines is to deliver large payloads across long distances in the shortest possible time or with the minimal energy expenditure. There are roads, airports, shipyards, and other foundations that support this transportation, enabling the structural design of cars, trains, planes, and ships to focus on transportation tasks. On the other hand, locomotion in nature is primarily for survival. Animals and insects have evolved to survive in various environments. Each species uses their mode of locomotion to hunt for food, find mates, and escape danger all in unstructured natural environments. Therefore, the requirements for biological locomotion are much more complicated than human transportation systems.

Biomimetic robots try to mimic the structural characteristics and the principles of movement to be able to move around places where conventional machines or robots are unable to perform as needed. Animals can crawl on a rugged terrain at a high speed, can climb walls without a tether, can fly in cluttered environments and hover and perch as needed.

Depending on the size of the species the optimal mode of locomotion and the underlying structure is different. For example, jumping is found frequently in small insects to escape danger, since their small size makes it hard for them to escape quickly using other forms of locomotion. Jumping by a large animal is different from jumping by small insects like a flea. Larger insects or animals tend to use their legs to run or crawl to escape the danger. Large birds flap their wings at a much lower frequency, and use gliding mode whereas bees and flies beat their wings continuously at a high frequency during flight. The structure is very differ-

ent, where the wings of a bird have bones, muscle, and feathers versus the muscle-less and lightweight wings of insects. Therefore, when developing biomimetic robots, the size of the target species should be taken into account.

Since nature has evolved to survive in extreme environments, there are many examples of extreme locomotion that are typically not possible with conventional engineering designs. For example, the wall climbing robot Stickybot uses the directional adhesion principle of a gecko to climb up smooth vertical walls. However, directional adhesion alone is not enough. The design has to enable even pressure distribution on the pad to make sure the pads are well in contact with the wall. These small details can be important to performance of biomimetic robots and should be considered carefully.

Since robots are commonly built to perform tasks too tedious or dangerous for humans, it is natural to adopt designs found in nature for functionality where nature has already found a solution. In fact, many robot designs in this handbook, such as legged robots and robot hands and many examples of flying robots, underwater robots, and micro robots, are biomimetic. This chapter will focus on areas of biomimetic robot designs that have been recently expanding. Legged robots and robot hands have already formed large communities and are covered in separate chapters. There are various other forms of locomotion, e.g., crawling, jumping, swimming, and flapping, that are being researched to mimic the principle of movement and the biological structure. The structure and the components of these robots will be reviewed and discussed in this chapter.

23.2 Components of Biomimetic Robot Design

Biomimetic robot design begins with an understanding of the underlying principles at work in a natural system.

For the design of a biomimetic robot, the components used in building the robot are important; the structural

design is constrained or enabled by the actuator system, the materials and the fabrication methods used to build the robot.

Understanding of the principles of movement found in nature initiates the design of biomimetic robots. This can be studied by observing the kinematics and measuring forces in moving animals, or by understanding and modeling the dynamics. Substantial research on biological locomotion analyzes the kinematics of the animal. However, it is important to understand the dynamics behind the kinematics to be able to implement the dynamic principles into the robot design, which will enable the robot to perform like an animal, instead of just looking like one. *Full* et al. proposed clock-driven, mechanically self-stabilizing, compliant sprawled-posture mechanics to explain a cockroach racing seemingly effortlessly over a rough surface [23.1, 2]. *Ellington* built a system that can measure the force generated by flapping wings to understand the thrust generated by insect wings [23.3]. These studies in biology have influenced robotics researchers, and inspired them to build hexapod and flapping-wing robots.

To implement biological principles in engineered systems, components that can create performance similar to that of nature is required. Nature's biological structures are composed of various materials, e.g., tissues, bones, cuticles, flesh, and feathers. These materials are replaced with engineered materials, e.g., metal, plastics, composites, and polymers. New engineered materials are being developed that exhibit similar properties to natural materials, which will enable life-like robots. However, the performance of the biomimetic robot can be similar to nature without actually mimicking the exact structure. Therefore, it is important to decide to what level biomimicry is re-

quired. Large robots tend to be built with conventional mechanical components such as motors, joints, and linkages made of metal. The challenge is in building meso-scale robots, where the conventional mechanical components become ineffective, due to friction and other inefficiencies. As the robot becomes smaller, it is beneficial to mimic not just the kinematics seen in nature, but also the structure at the component level. Another challenge for small scales is actuation – the actuator must be as effective as the muscle even at small scales.

A number of new manufacturing methods have become available which also enable new designs that were not previously possible by more classical machining methods and *nuts-and-bolts* assembly techniques. Examples include shape deposition manufacturing and smart composite microstructures. In many cases, these new fabrication processes facilitate the construction of novel biomimetic robots beyond what was possible by conventional means.



Levels of mimicry can vary depending on the components used in the design. The robot can simply look like an animal, but not perform similarly to the mimicked animal. On the other hand, once the principle is mimicked the robot does not have to look like the animal, but it can still perform a task in a similar manner as the animal. The different ways of mimicking allows each robot to have its own characteristic. For example, a flea uses what is called a torque reversal for jumping, which is a unique method of storing and releasing large amount of energy. In nature, this method is possible with muscles and a lightweight-legged structure. To mimic the flea's locomotion, we need an actuator that is comparable to muscles and a fabrication method that allows us to build a small-scale rigid structure.

23.3 Mechanisms

Developing multilegged robot has been achieved by using specific design which enables some function or biomimetic model inspired by multilegged insects. Especially, the ability of a cockroach enabling to run on a rough surface at a high speed has inspired to develop a series of multilegged robots. They are capable of maintaining stability during locomotion at a high speed (relative to their body length).

23.3.1 Legged Crawling

Some types of cockroaches can achieve speed up to 50 body length per second and can crawl on uneven terrain, overcoming obstacles far higher than their height [23.2]. RHex (Fig 23.1a) [23.4] is one of the

first robots to implement cockroach-like characteristics. It is a hexapod crawling robot with C-shaped legs, so it is suitable for walking on uneven terrain or large obstacles, as shown in  VIDEO 400. Mini-Whegs (Fig 23.1b) [23.5] also have unusual wheel with three spokes. Because of the wheel-spoke structure, the gait passively adapts to the terrain similar to climbing cockroaches, as shown in  VIDEO 401 [23.15]. Sprawlita (Fig 23.1c) [23.6] is a hexapod crawling robot that uses pneumatic actuators on each leg and passive rotary joints so that it can achieve dynamic stability. It weighs 27 kg and its speed is over 3 body length/s or 550 mm/s. iSprawl (Fig 23.1d) [23.7] is hexapod crawling robot that uses extension of each legs during crawling. This robot is driven by electric motors and

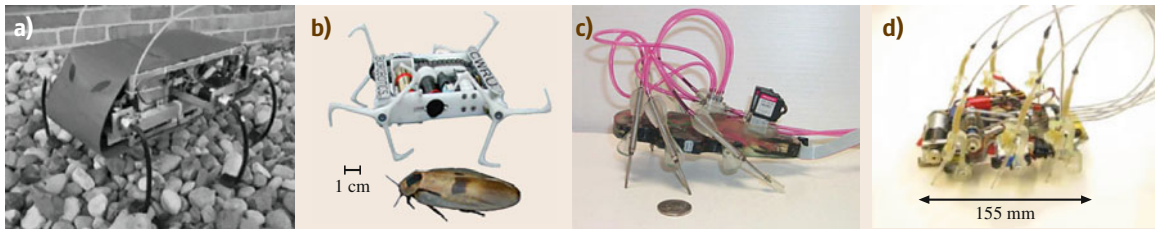


Fig. 23.1a–d Crawling robots inspired by cockroach (a) RHex (after [23.4]), (b) Mini-Whegs (after [23.5]), (c) Sprawlita (after [23.6]), (d) iSprawl (after [23.7])

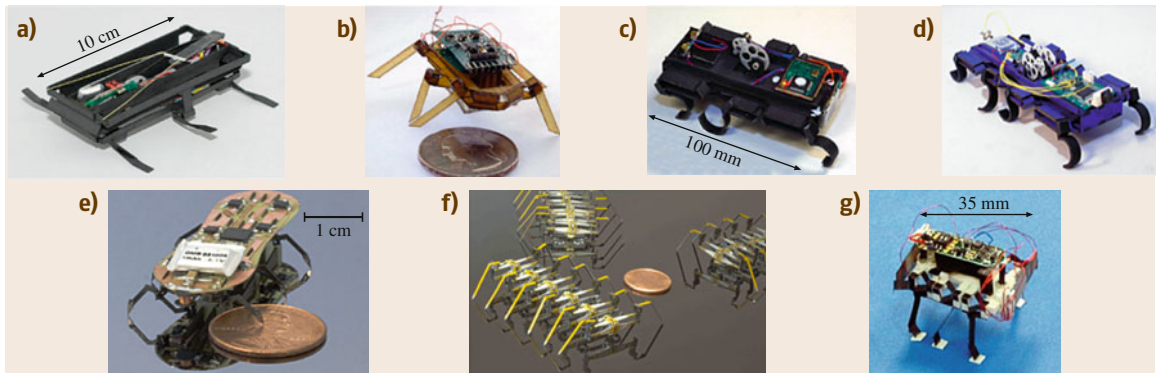


Fig. 23.2a–g Crawling robots inspired by cockroach. (a) DASH (after [23.8]), (b) RoACH (after [23.9]), (c) DynaRoACH (after [23.10]), (d) OctoRoACH (after [23.11]), (e) HAMR3 (after [23.12]), (f) centipede-like modular robot (after [23.13]), (g) crawling robot through the integration of microrobot technologies (after [23.14])

flexible push–pull cables. Rotation of the motor causes the legs to extend or contract. It weighs 300 g and is able to crawl 15 body length/s or 2.3 m/s, as can be seen in [VIDEO 403](#).

Cockroach-based designs would improve the performance of millimeter or centimeter scale crawling robots which face inefficiency with conventional mechanisms. DASH (Fig 23.2a) [23.8] is a hexapedal crawling robot fabricated using SCM (Smart composite manufacturing) process. This robot has only one electric motor coupled to a four-bar linkage pushing the legs in an elliptical crawling motion, as shown in [VIDEO 405](#). DASH weighs 16.2 g and achieves

speed up to 15 body length/s or 1.5 m/s. RoACH (Fig 23.2b) [23.9] is a hexapod crawling robot that imitate cockroach's alternating tripod gait. A typical cockroach gait involves the ipsilateral front leg, hind leg, and contralateral middle leg moving simultaneously. Two sets of three legs tread on a surface in turn – generating the *alternating tripod gait*. RoACH uses two shape memory alloy (SMA) wire actuators to contract the body in two orthogonal directions. Contraction of the two actuators results in motion of legs through a four-bar linkage. The legs repeatedly operate swing and stance motions according to the sequential stimulation of the two actuators and it can be seen in [VIDEO 286](#). It weighs 2.4 g and is able to crawl 1 body length/s or 3 cm/s. DynaRoACH (Fig 23.2c) [23.10] has six legs driven by one DC motor. It has passive dynamics similar to RoACH to achieve better locomotion performance. Lift motion is achieved by a slider crank mechanism and swing motion by a four-bar mechanism. Like RHex, it uses C-shape legs so that the robot has lower vertical stiffness, lateral collapsibility for obstacle climbing, and more distributed ground contact. It weigh 24 g and is 100 mm long and is capable of speeds up to 14 body length/s or 1.4 m/s. OctoRoACH (Fig 23.2d) [23.11] is quite similar to DynaRoACH, but it has two motors driv-

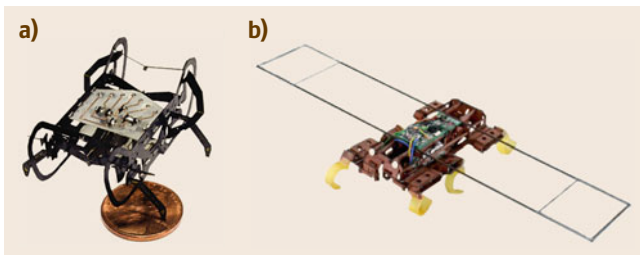


Fig. 23.3a,b The latest version of crawling robots which shows improved performance (a) HAMRV (after [23.16]), (b) VelociRoACH (after [23.17])

ing the legs on each side. It has eight legs so that it maximizes pitch stability using two motors. OctoRoACH weigh 35 g and is 100 mm long. HAMR3 (Fig. 23.2e) [23.12] uses nine piezoelectric actuators. Each leg performs swing and lift motion through two decoupled piezoelectric actuator through four-bar slider-crank mechanisms and spherical five-bar mechanisms (VIDEO 406). This robot weighs 1.7 g and has speeds up to 0.9 body length/s or 4.2 cm/s (4.7 cm long robot). Especially, the HAMR is manufactured using a method inspired by pop-up books that enables fast and repeatable assembly. Multilegged robots inspired by centipede using mechanism similar to alternative tripod gaits is also developed (Fig. 23.2f) [23.13]. Its several gait patterns that differ in gait frequency and phase are described in VIDEO 407. Using microrobot technologies developed until 2006, integrated structure was developed although the structure was not yet tested (Fig. 23.2g) [23.14].

With more experiments and research about motion of cockroaches, the cockroaches like robots can extremely improve their performance by revision using biomimetic model. HAMRV, which is the most recent version of HAMR [23.16], can move 10.1 body length/s (44.2 cm/s) which is remarkably improved compared to preceded versions are capable of running at 0.9 body length/s. It is even capable of maneuverability and control at both low and high speeds. VelociRoACH (Fig. 23.3b) [23.17] which is the latest version of RoACH can run 2.7 m/s extremely higher speed relative to previous version (VIDEO 408).

23.3.2 Worm-Like Crawling

Worm-like crawling motion can be separated into two categories: peristaltic crawling and two-anchor crawling. Worms exhibiting peristaltic crawling locomotion – such as earth worms – can move through small tunnels with limited space. Therefore, mimicry of this locomotion imposes similar characteristics to the robot and it has the potential to be used in small and harsh environment such as collapsed disaster site or inside a pipe line. which A schematic of peristaltic locomotion is shown in Fig. 23.4. By sequentially changing the volume of the body, the whole structure generates the moving motion.

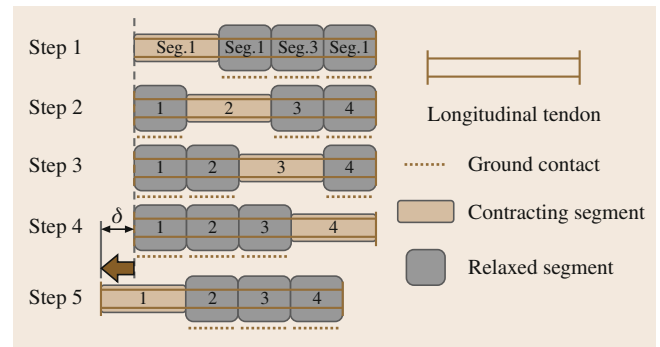


Fig. 23.4 Peristaltic locomotion (after [23.19])

The key design issue in mimicking peristaltic motion is how to create sequential volume change. Many researchers have tried various creative methods to solve this problem. *Boxerbaum* et al. built a robot with a mesh structure, and using a single motor and wire, made a partial volume change of the robot which realized a crawling motion (Fig. 23.5a) [23.18]. *Seok* et al. used a SMA coil spring actuator to change the segmented volume, and also used a mesh tube as the body structure (Fig. 23.5b) [23.19]. *Menciassi* et al. also used a SMA coil spring actuator, but they used a micro hook to enhance the friction force (Fig. 23.5c) [23.20].

Two-anchor crawling is a locomotion method used by inchworms. This locomotion mode is not fast, but it can overcome nearly any complicated topology. With an appropriate gripping method, it not only can climb vertical walls, but also can cross gaps. There are two key design issues for generating a two-anchor crawling motion: the first is how to change the shape of the waist and the second is how to anchor and unanchor to the surface. *Kotay* and *Rus* simply used an electric motor to articulate the waist motion and used an electromagnetic pad as the anchoring method (Fig. 23.6a) [23.21]. Using an electromagnetic pad, the robot can climb a steel structure. *Cheng* et al. used a tendon-driven mechanism with a compressible body and an anisotropic friction pad to generate motion (Fig. 23.6b) [23.22]. Using symmetrical or asymmetrical winding of the wire attached on the both side, the robot can make forward or steering movements. *Koh* and *Cho* used SMA coil spring actuators to control the waist motion (Fig. 23.6d) [23.23].

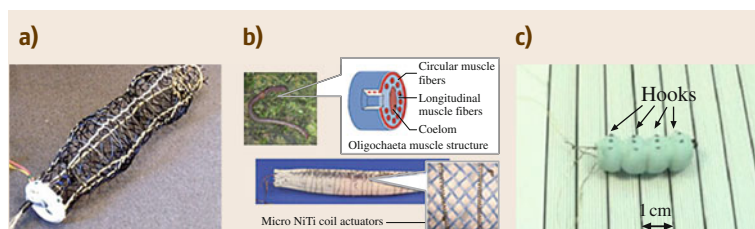


Fig. 23.5 (a) Robot with peristaltic motion (after [23.18]). (b) Meshworm robot (after [23.19]). (c) Biomimetic miniature robotic crawler (after [23.20])

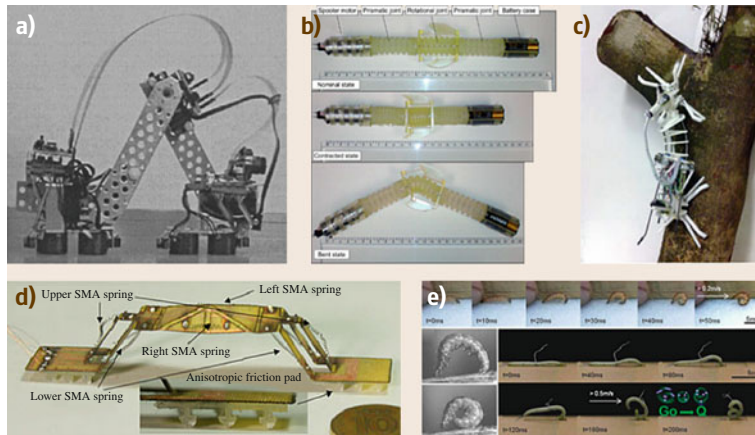


Fig.23.6a–e Two anchor crawling robot. (a) The inchworm robot (after [23.21]). (b) The soft mobile robot with thermally activated joint (after [23.22]). (c) Treebot (after [23.24]). (d) Omega shaped inchworm inspired crawling robot (after [23.23]) (e) GoQBot (after [23.25])

The body of the robot is made by a single sheet design with glass fiber composite, and a folding pattern designed to enable steering motion even though the robot was built by a single sheet. *Lin et al.* realized a robot with two-anchoring motion, but he also added a rolling locomotion to solve the speed limitation of previous two-anchor motion demonstrations (Fig. 23.6e) [23.25]. *Lam and Xu* realized another method to generate the waist motion. The robot used a backbone rod coupled to an electrical motor. By controlling the length of the backbone using the motor, the robot can control the position of the anchoring point (Fig. 23.6c) [23.24].

23.3.3 Snake Robots

Studies on the locomotion of snakes began in middle of the 20th century [23.30–32]. Snakes are limbless, slender, and flexible [23.33]. Their locomotion gives them adaptability and mobility through land, uneven ground, narrow channel, pipes, and even water, and even flying between trees [23.34, 35]. An advantage of snake-like locomotion is the great versatility and freedom of movement with numerous degrees of freedom [23.36]. Additionally, snake locomotion could be efficient compared to legged animals, because there is no lifting of the center of gravity or limb acceleration [23.37]. In 1970s, *Hirose* developed a continuous locomotion model and a snake-like robot called the *Active Cord Mechanism* (ACM) [23.38]. After the *Hirose's* ACM robot, snake-like robots have been widely studied. In 1972, ACM-III (Fig. 23.6) was developed and it was the first robot that mimics the serpentine motion of real snakes [23.38]. The recent versions of ACM are in VIDEO 397.

Locomotion of snake-like robots can be categorized into the following different types: serpentine motion, sinus lifting, pedal wave, side-winding, spiral swimming, lateral rolling, lateral walking, mixture lean serpentine, and lift rolling motions.

The first generation of snake-like robots could only achieve motion on planar surfaces. These designs quickly evolved and current snake-like robots can go upward within narrow pipes and can climb and hold on to trees like VIDEO 393 [23.39]. To facilitate traversing large obstacles, some robots have added actuated articulation between each joint [23.40]. In addition, there are some snake-like robots that can swim in water. With a firmly waterproofed body, these robots can swim with spiral and sinusoidal locomotion patterns [23.38].

Today, mechanism design of snake-like robots can be classified with following five different types: active

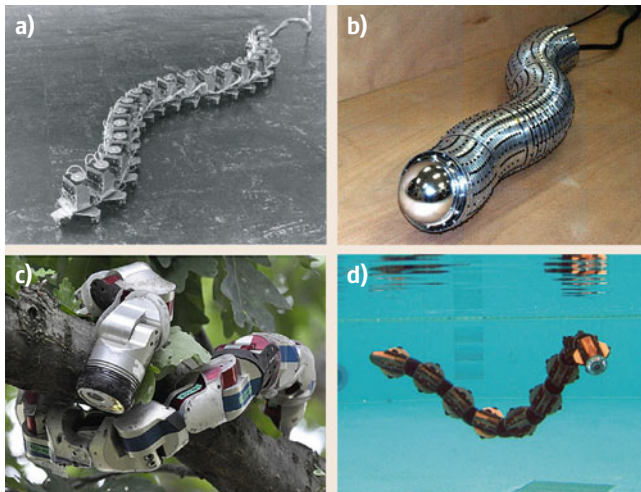


Fig.23.7a–d Three snake-like robots. (a) AMC-III, Shigeo Hirose, Fukushima Robotics Lab, Tokyo Institute of Technology (after [23.26]), (b) Slim Slime Robot II (SSR-2), Shigeo Hirose, Fukushima Robotics Lab, Tokyo Institute of Technology (after [23.27]), (c) Modular snake robot, Howie Choset, Biorobotics Lab, Carnegie Mellon University (after [23.28]), (d) AMC-R5, Shigeo Hirose, Fukushima Robotics Lab, Tokyo Institute of Technology (after [23.29])

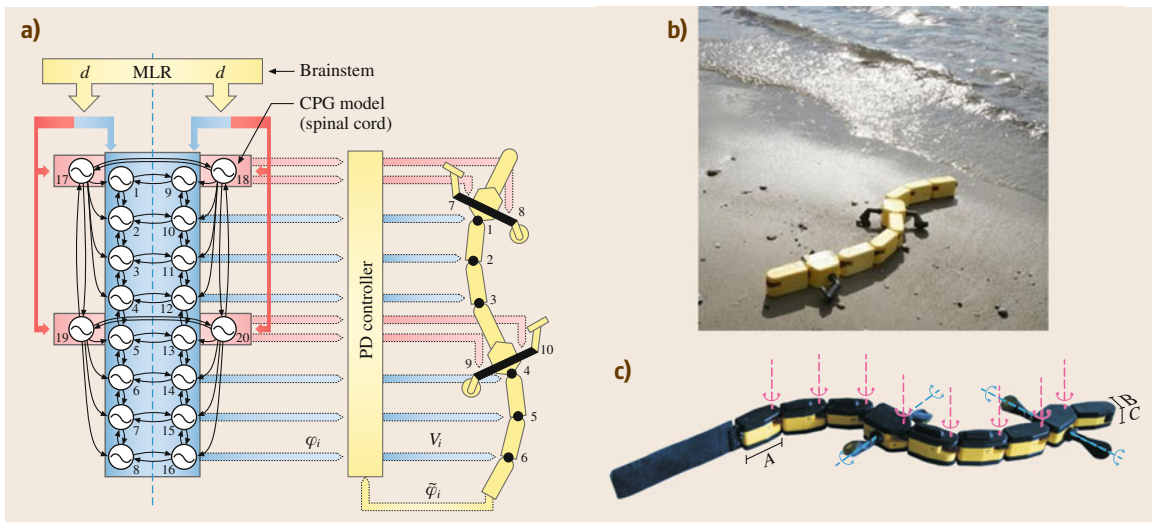


Fig. 23.8 (a) Configuration of the CPG model (after [23.41]). (b) Salamandra robotica I, Auke Jan Ijspeert, Biorobotics Lab, Ecole Polytechnique Federale de Lausanne (after [23.41]). (c) Salamandra robotica II, Auke Jan Ijspeert, Biorobotics Lab, Ecole Polytechnique Federale de Lausanne (after [23.42])

bending joint type, active bending and elongation joint type, active bending joint and active wheel type, passive bending joint and active wheel type, and active bending joint, and active crawler type [23.43]. Each of these types of snake-like robots consist of a number of serially connected joints. Therefore, snake-like robots are easy to modularize with their joints [23.43].

Most snake-like robots are equipped wheels that are actively or passively driven. Recently, wheelless snake-like robots have been studied [23.32]. These robots move with undulatory motion, especially lateral undulation that can be observed in real snakes. Some snake-like robots are actuated with smart materials, such as shape memory alloys and IPMCs, rather than motors [23.44]. Snake-like robots roll to avoid obstacles and interact with environment. They make waveforms with their body for propulsion. Therefore, it is important to define the configuration of the body of the robots. Measuring yaw (pitch) and roll angles are important for controlling the snake robots. Tilt sensors, accelerometers, gyroscope, and joint angle sensors are typically leveraged to control the robot [23.37]. Tactile sensors attached to the contact area or outside of the body of the snake-like robots have been used to measure surface contact forces at each joint, providing more information to the controller. Additionally, measuring contact forces could be useful for active and adaptive grasping of the snake-like robot [23.45].

However, due to the high degrees of freedom of the snake-like robots, designing controllers is not easy even for flat surface locomotion. Efforts without complex sensors and controllers are in [VIDEO 392](#). Because of

this, contrasting with the advantages of locomotion of real snakes – which can move in uneven environments – most existing snake-like robots are developed based on flat surface movement [23.46].

A major motivating application for snake-like robots is the exploration of hazardous environment that are inaccessible to humans. In particular, industrial inspection of pipes and ventilation tubes, and chemical channels are key operating environments. There is also the potential for snake-like robots as medical devices, such as minimal invasive surgery device and laparoscopy and endoscopy [23.37]. For these applications, snake-like robots require their outer skin to hermetically seal the internal components [23.40].


There are numerous challenges for snake-like robots. For greater reliability, robustness and controllability, the mechanisms and configuration of the snake-like robots could be simplified. To use the snake-like robots for exploration and inspection applications, routing of external wires for electronics and power to the robot is an important consideration. Finally, with a large number of degrees of freedom typical of snake-like robots, designing efficient control strategy is large issue [23.37].

Similar to undulatory locomotion of snakes, body of salamanders makes S-shape standing waves. They are capable of rapidly switching between swimming and walking locomotion. Their locomotion in aquatic and terrestrial environments is generated by a central pattern generation (CPG) and stimulation of a mesencephalic locomotor region (MLR) located in the mid-brain (Fig. 23.7 and [VIDEO 395](#)) [23.41]. There were

some efforts to produce similar swimming and walking gaits to real salamander with robotic salamanders. The salamander robots with the mathematical CPG model, DC motors, and oscillators could produce similar kinematics to real salamanders [23.42] (Fig. 23.8).

23.3.4 Flapping-Wing Flight

Flapping-wing flight is a common inspiration for biomimetic aerial robots. This is due to the agility of natural flyers such as birds, bats, and insects. Advances in the understanding of the aerodynamics of flapping-wing based on hydrodynamic theories and experimental results have provided insights into thrust production in flapping-wing animals [23.47]. From observation of the flapping motion exhibited by insect flight, the translational, and rotational motions of the wing produce lift forces at high angles of attack – beyond what is typical for fixed wing aircraft. The formation of a large vortex at the leading edge of the wing and the recapturing of shed vortices by properly timing of the swing enhance the resultant lift force [23.48]. Figure 23.9 shows the representative motion of an insect wing during flight and the vector formation of hydrodynamic forces. Such characteristics learned from nature inspires the design of wing-driving systems in flapping-wing flying robots.

Most flapping mechanisms are constructed from electromagnetic rotary motors driving crank-rocker linkages to flap the wings. Examples include the DelFly II [23.49], Robot dragonfly [23.50] and Nano Hummingbird [23.51] as shown in Fig. 23.10. As can be seen in  VIDEO 402, DelFly II employs four-wing morphology where two wings on each side perform

a *clapping* motion during each period. This contributes to lower power consumption and the low rocking amplitude of the fuselage. The DelFly II model used a crank mechanism such that the gear axis is perpendicular to the flying direction, for overcoming phase differences between the two sets of wings and this difference induced rotational movement on the fuselage [23.49]. In related work, the Robot Dragonfly [23.50] is inspired from a dragonfly's hovering capabilities and utilizes a tandem wing model. Each transmission link is attached to gear mechanisms that can make wing motions similar to those of a dragonfly. The Nano Hummingbird uses single pair of flapping wings as with real hummingbirds. The flapping mechanism is a dual lever, string-based flapping mechanism. Wing rotation modulation for control of the wing attack angle is achieved by the two adjustable *stops* which limit how far each wing can rotate [23.51]. Alternative mechanisms use oscillating actuators and flexure-based transmissions systems (these mechanisms are discussed in Sect. 23.4.2).

As the robot scale decreases, previous flapping mechanisms have been difficult to adapt due to manufacturing challenges and the physics of scaling. The Harvard robotic fly shows promising fabrication and design processes to build the small scale flapping air vehicle as shown in Fig. 23.11 [23.52]. Previous versions of the Harvard robotic fly had three degrees of freedom, only one of which was actuated. The angle of attach of two the wings are passively controlled by a compliant flexure joint connected to the transmission. The wing beat frequency is tuned at 110Hz in resonance. Through advances in meso-scale manufacturing methods, the capabilities of the robotic fly have been dramatically extended and unconstrained flight

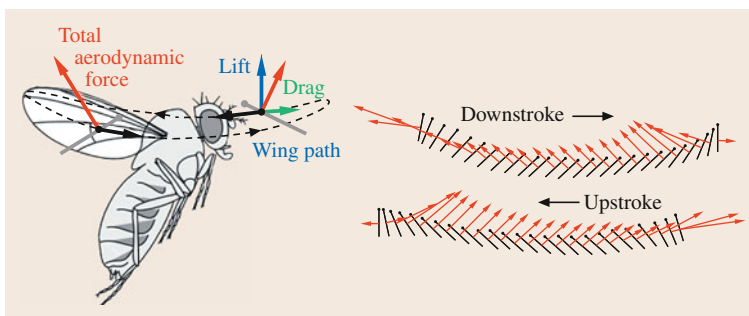


Fig. 23.9 Diagram of wing motion indicating magnitude and orientation of the aerodynamic force (after [23.48])

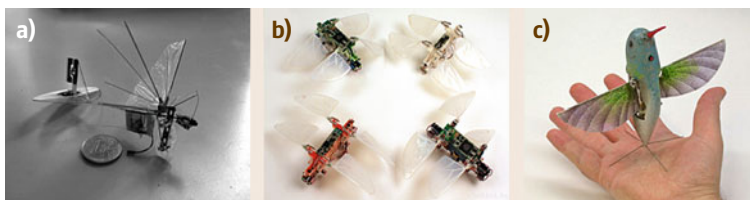


Fig. 23.10 (a) Delfly II (after [23.49]), (b) Robot Dragonfly [23.50], (c) Nano Hummingbird (after [23.51])

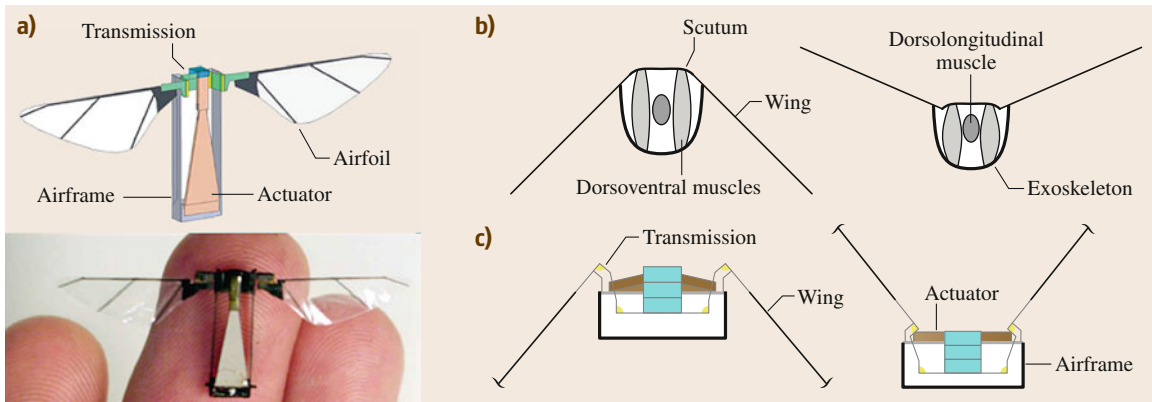



Fig. 23.11 (a) Harvard robotic fly, (b) Illustrations of thorax mechanisms, (c) and transmission (after [23.52])

has been demonstrated like  VIDEO 399 in an 80 mg robot as discussed in Sect. 23.4.2.

Flapping-wing locomotion can also be extended to multimodal locomotion in combination with other mechanisms. In the DASH+Wings shown in Fig. 23.12 [23.53], the combination of wing flapping and crawling compliments each other for improving agility and stability. This hybrid robot improves performance of the maximum horizontal running speed in a factor of two and the maximum climbing incline angle by a factor of three.

23.3.5 Wall Climbing

Climbing and maneuvering on vertical surfaces present a difficult challenge. However, this locomotion mode is needed in many areas such as shipping, construction, and terrestrial locomotion in natural environment. Early attempts involved the use of suction cups, magnets,

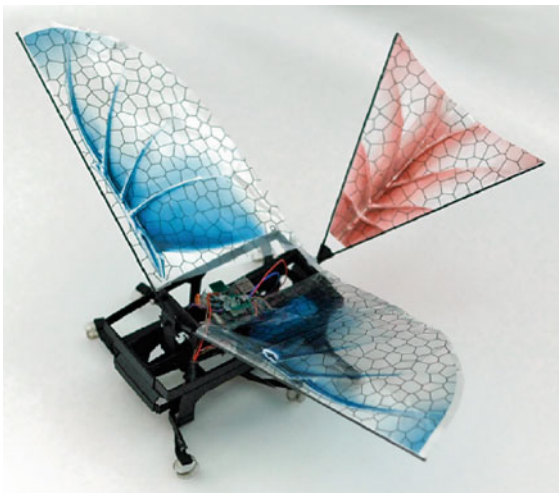



Fig. 23.12 DASH+Wings (after [23.53])

or pressure-sensitive adhesives to implement climbing. More recently, claw, spines and sticky pads inspired by nature have been used. Climbing insects and animals inspired many researchers. Insects and reptiles employ small spines that catch on fine asperities. Geckos and some spiders employ large numbers of very fine hairs that achieve adhesion based on van der Waals interaction.

Early in the 1990s, nonbiomimetic wall climbing robots, i.e., the Ninja-1, RAMR, and Alicia were developed using suction cup. Ninja-1 attaches to a wall making use of a suction mechanism (Fig. 23.13a). The main mechanism consists of a three-dimensional (3-D) parallel link, a conduit-wire-driven parallelogram, and valve-regulated multiple sucker that enabled the robot to attach the surface with grooves [23.54]. RAMR used underactuation to remove the redundant actuators to drive the small two-legged robot [23.59]. The Alicia robot was developed for a variety of applications such as maintenance, building inspection, and safety in process and construction industries. An aspirator is used to depressurize a suction cup, so the whole robot can adhere to the wall like a standard suction cup. The Alicia3 robot use three of the Alicia II modules, allowing the whole system to better deal with obstacles on the target surface [23.60]. REST is an exceptional case that applies electromagnets instead of suction cup. It climbed only ferromagnetic wall using electromagnetic four legs with 12-DOF [23.61].

The effective wall climbing mechanisms of animals and insects have inspired development of biomimetic wall climbing robots. Typical robots utilizing bio-inspired spines found in climbing insects and cockroach are Spinybot and RiSE. Spinybot in  VIDEO 388 climbs hard vertical surfaces including concrete, brick, stucco, and masonry with compliant microspine arrays (Fig. 23.13b). It can exploit small asperities (bumps or pits) on the surface. The sequence of motions is

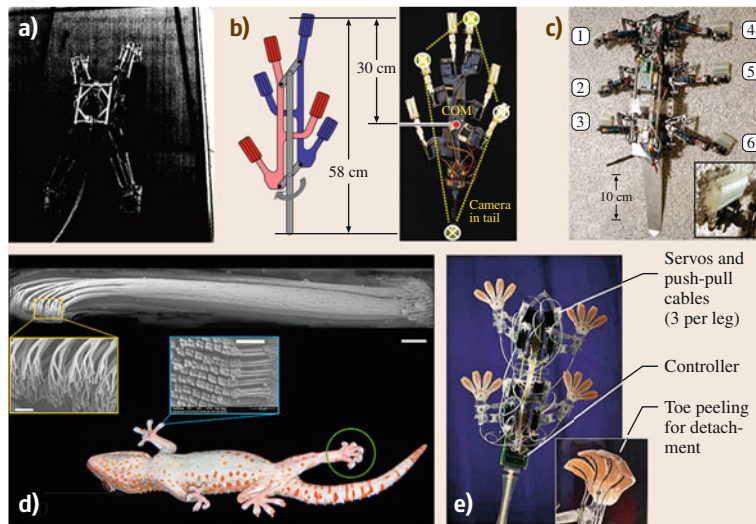


Fig. 23.13 (a) Ninja-1 (after [23.54]), (b) Sphero II (after [23.55]), (c) RiSE (after [23.56]), (d) Gecko adhesive system (after [23.57]), (e) Stickybot (after [23.58])

accomplished using an under-actuated mechanism consisting of a single rotary RC servo motor and several spines independently engaging asperities on the concrete surface [23.55]. RiSE is a hexapod robot capable of locomotion on ground and vertical surfaces such as brick, stucco, crushed stone, and wood, as shown in [VIDEO 390](#) (Fig. 23.13c) [23.56]. To climb a vertical wall, it uses microspines inspired by cockroach's tarsus structure. In addition, it held its center of mass close to surface to minimize the pitch-back moment. RiSE also employed a static tail to reduce disparity from the pull-in forces experienced by the different legs [23.56, 62].

Insects and geckos can provide inspiration for novel adhesive technology and for the locomotion mechanisms employed during climbing. Geckos are able to climb rapidly up smooth vertical surfaces and biologists reveal that a gecko's foot has nearly five hundred thousand keratinous hairs or setae. And measured adhesive force values show that individual seta operate by van der Waals forces. The gecko's toe uncurling and peeling suggests that two aspects of setal function increase effectiveness [23.63]. The subsequent study shows that the linear relation between adhesion and shear force is consistent with a critical angle of release in live gecko toes and isolated setal arrays (Fig. 23.13d). And the frictional adhesion model provides an explanation for the very low detachment forces observed in climbing geckos that does not depend on toe peeling [23.57].

Stickybot, Mini-Whegs, Geckobot, and Waalbot are prototypical robots that leverage biomimetic dry adhesives. Stickybot climbs smooth vertical surfaces such as glass, plastic, and ceramic tile at 4 cm/s, as shown in [VIDEO 389](#) (Fig. 23.13e). The robot employs several design principles adapted from the gecko including a hierarchy of compliant structures, directional adhe-

sion. The undersides of Stickybot's toes are covered with arrays of small, angled polymer stalks. They readily adhere when pulled tangentially from the tips of the toes toward the ankles. When pulled in the opposite direction, they release [23.58]. Mini-Whegs uses wheel-legs with compliant, adhesive feet for climbing. The foot motion mimics the foot kinematics of insects, in order to test new bio-inspired adhesive technologies and novel, reusable insect-inspired polymer (polyvinylsiloxane) [23.67]. Geckobot has kinematics similar to a gecko's climbing gait. It uses a novel peeling mechanism of the elastomer adhesive pads, steering mechanisms and an active tail for robust and agile climbing [23.68, 69]. Waalbot used two actuated legs with rotary motion and two passive revolute joints at each foot. The robot has ability to climb on nonsmooth surfaces as well as on inverted smooth surfaces using gecko-like fibrillar adhesives and passive peeling. It is also capable of plane-to-plane transitions and steering to avoid obstacles [23.70].

Different approaches for climbing include electroadhesion. Electroadhesives use a novel clamping technology called compliant electroadhesion – a form of electrically controllable adhesion. This involves inducing electrostatic charges on a wall substrate using a power supply connected to compliant pads situated on the moving robot. This generates high clamping forces that are around 0.2–1.4 N supported for a one square centimeter clamp area, depending on the substrate. Regarding power considerations for electroadhesion, assuming 50% conversion efficiency, in the worst-case scenario, two AAA batteries weighing 7.6 g each can hold up a robot in *perch* mode for almost one year. Electroadhesion combined with a conventional wheeled robot results in inchworm-style wall climbing [23.79].

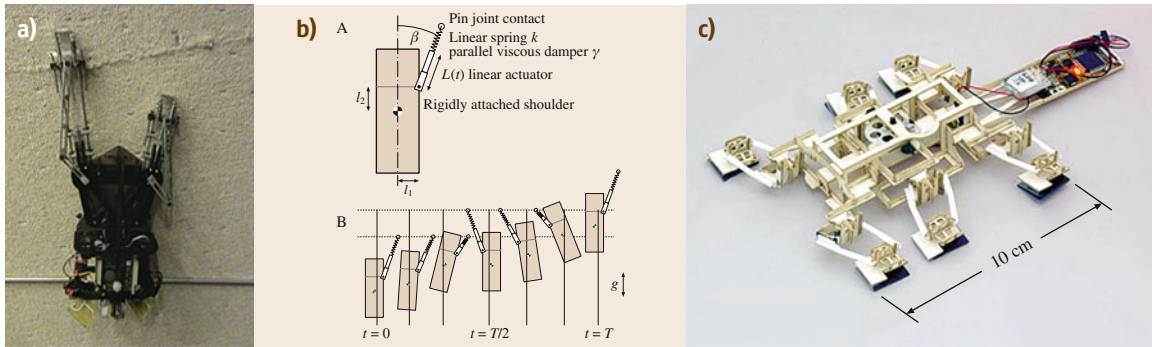


Fig. 23.14 (a) DynoClimber (after [23.64]). (b) A dynamic template for climbing (after [23.65]). (c) CLASH with gecko pad (after [23.66])

Dynamic wall climbing is the next challenge for wall climbing robots because previous robots were slow and in most instances restricted to targeted surfaces. For dynamical climbing originating in biology, pendulous climbing model was proposed (Fig. 23.14b). This model abstracts remarkable similarities in dynamic wall scaling behaviour exhibited by radically different animal species such as cockroaches and geckos [23.65]. The findings suggest that animals employ large lateral in-pulling forces and body rotations to achieve fast, self-stabilizing gaits. DynoClimber displays the feasibility of adapting the dynamics to robot that runs vertically upward (Fig. 23.14a). A novel bi-pedal dynamic climber can scale a vertical wall fast accompanying while achieving dynamic stability. For dynamic climbing, this robot consists of a DC motor, a crank slider mechanism and passive-wrist springs so its climbing at speeds 0.67 m/s (1.5 body lengths/s) [23.64]. The climbing robot CLASH has modified DASH platform but it actuates in horizontal direction to reduce height (7 mm from robot bottom). One of the key points is passive foot mechanism. When climbing upward, the foot hangs its spines on the surface and then retracts passively. This increases the shear and normal forces and enables climbing on loose cloth at 15 cm/s speed, as shown in [VIDEO 391](#) [23.80]. The next version of CLASH has a foot that consists of an 18×15 mm pad of microfabricated PDMS (polydimethylsiloxane) ridges inspired by gecko feet (Fig. 23.14c). The ankle is an isosceles-trapezoid four-bar that creates a remote center-of-motion. This mechanism allows the foot to make coplanar contact with the surface and reduces roll peeling moments [23.66].

23.3.6 Swimming

Underwater vehicles have been made to achieve marine explorations, surveillance, and environmental monitoring. Most underwater vehicles employ propellers for

propulsion and these vehicles have shown great performance with respect to the cost of transport. However, efficiency and manoeuvrability in confined areas is problematic for most surface or underwater vehicles. Moreover, propeller-driven vehicles risk tangling when moving through environments with debris and vegetation. To resolve these issues, researchers have tried to replace the conventional rotary propellers with undulatory movement inspired by fish (Fig. 23.15).

The undulatory movement of fish provides two main advantages – manoeuvrability in confined areas and high propulsive efficiency. The main difference between existing propeller and undulatory movement is turning radius and speed. Fish can turn with a radius 1/10 of their body length, while propeller-driven ships require a much larger radius. Accordingly, the turning speed of fish is much faster than ships. Beyond manoeuvrability, the driving efficiency in biological swimmers also show more improvement over man-made systems [23.81].

To achieve fish-like swimming motion, various mechanisms have been employed such as linkage mechanisms and compliant mechanisms. *Barrett* first proposed a RoboTuna by using six servo motors and eight linkages [23.71]. *Morikawa* et al. built a robotic fish mimicking the caudal musculo-skeletal structure of a tuna with two rubber pneumatic artificial muscles and a multijoint bending mechanism [23.82]. A robotic dolphin was designed with four links and six servo motors to mimic the dorsoventral movement of a real dolphin [23.83]. *Low* developed a fish robot to generate arbitrary undulating waveforms, by connecting ten servo motors in series by linking them with sliders [23.74]. *Liu* and *Hu* developed a robotic fish mimicking the body motion of carangiform fish by using three servo motors on each joint, as shown in [VIDEO 431](#) [23.72]. *Yang* et al. presented Ichthus V5.5 by using 3-DOF serial link-mechanism with servo motors on each joint for propulsion, as shown in [VIDEO 432](#). Ichthus V5.5 has

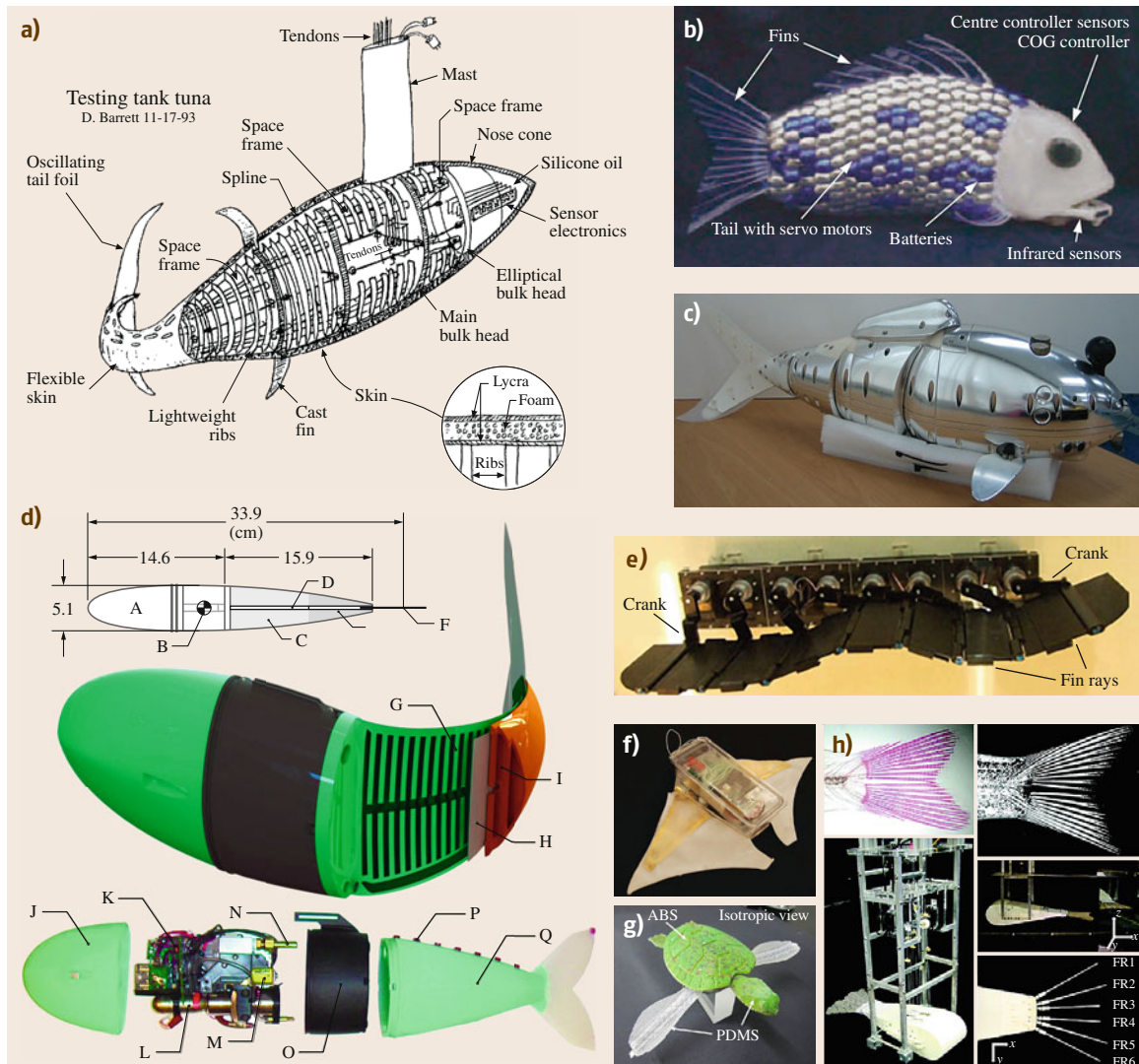


Fig.23.15a–h Design of robotic fin (a) Robo Tuna (after [23.71]), (b) G9 serise robotic fish (after [23.72]), (c) Ichthus (after [23.73]), (d) Undulating robotic fin rays (after [23.74]), (e) Soft robotic fish (after [23.75]), (f) Robotic mata ray (after [23.76]), (g) Turtle-like swimming robot (after [23.77]), (h) Robotic fin rays (after [23.78])

several sensors to navigate autonomously in the real environment such as rivers [23.73].

Beyond linkage mechanisms, several researchers have employed compliant materials in their designs to make the undulatory motion without complicated linkage structures. *Salumäe* and *Kruusmaa* implemented swimming kinematics of a trout by simply adjusting the compliance of a flexible fin with a single actuator [23.84]. *Alvarado* and *Youcef-Toumi* designed a robotic fish with a simple and robust mechanism, using a compliant body that was approximated by a continuous cantilever beam to generate a fish-like oscillating motions [23.85]. This simple design achieved

biomimetic locomotion using only one servomotor, while most other robotic fish use several motors to achieve biomimetic modes of swimming. *Marchese* et al. employed a compliant body with embedded actuators and used a novel fluidic actuation system that drives body motion, as shown in [VIDEO 433](#) [23.75]. *Park* et al. presented a guideline for optimizing the fin to maximize the thrust generated by a compliant fin. The *half- π phase delay* condition describes the condition that the thrust is maximized regardless of the shape of the fin, driving frequency, and amplitude. They also presented a variable-stiffness flapping mechanism to improve the performance of a compliant fin while



Fig.23.16a,b Escapement cam mechanism (a) Grillo (Ver.1) (after [23.86]) and (b) 7 g jumping robot (after [23.87])

the operating conditions change [23.88]. Tendons were used to vary the stiffness and the attachment point is determined based on the anatomy of a dolphin's fluke. Several fish robots that use smart actuators to create undulating motion have also been investigated [23.89]. Wang et al. embedded shape memory alloy (SMA) wire actuator to create flexible bending and investigated the musculature of a cuttlefish fin to aid the design of the biomimetic fin [23.90]. Chen et al. mimicked manta ray by using ionic polymer-metal composite (IPMC) as artificial muscles. They embedded an IPMC muscle in each pectoral fin and a passive PDMS membrane to lead to an undulatory flapping motion on the fin, as shown in [VIDEO 434](#) [23.76]. Kim et al. [23.77] used a smart soft composite (SSC) structure to generate bending and twisting motions in a simple, lightweight structure. Lauder et al. designed a robotic fish caudal fin with six independently moving fin rays based on the anatomy of bluegill sunfish and presented that the cupping motion produced greater thrust than others such as W-shaped, undulation, and rolling [23.78]. They used five different sets of fin rays and measured thrust by varying the motion program. In addition, Lauder et al. used a flexible plastic foil to explore the effects of changing swimming speed, foil length, and shape of the foil-trailing edge on undulatory locomotion [23.91].

23.3.7 Jumping

In nature, many animals use jumping as a locomotion strategy. Jumping has the advantages of overcoming large obstacles and avoiding predators quickly and increasing the chances of survival. Robots also experience challenges in overcoming obstacles larger than the characteristic dimension of the robot. To find solutions for this, many researchers have developed jumping robots inspired by nature.

The jumping process requires large amounts of energy to be released instantaneously. However, muscle has limited reaction speed – achieving a maximum acceleration of 15 m s^{-2} . Therefore, many small creatures, such as insects, have adapted special elastomers for energy storage to generate large accelerations in-

stead of using muscles. On the other hand, most large creatures, such as human that have relatively long legs, primarily use large muscles that can generate sufficient large force to swing long legs quickly.

In small-scale jumping, to achieve large instantaneous acceleration, the jumping process has two steps: 1) slow energy storage and 2) rapid release of the stored energy. Escapement cam mechanism is widely used to achieve these two steps. It consists of a spring, a radius varying cam, a motor, and a gearbox for torque amplification. The motor rotates the cam slowly, but powerfully, toward the direction of compressing or extending the spring. At the final portion of the cycle, the cam's radius returns to the initial state instantly, releasing the spring causing the robot to jump. Grillo (Ver.1) (in [VIDEO 278](#)) [23.86] and a similar 7 g jumping robot (in [VIDEO 279](#)) [23.87] use this escapement cam mechanism (Fig. 23.16).

A toothless gear mechanism is similar to the escapement cam mechanism. The main differences are that the toothless gear mechanism uses an incomplete gear instead of a change in the cam shape. The motor actuates the incomplete gear, and the gear actuates a transmission to compress or extend a spring. When the

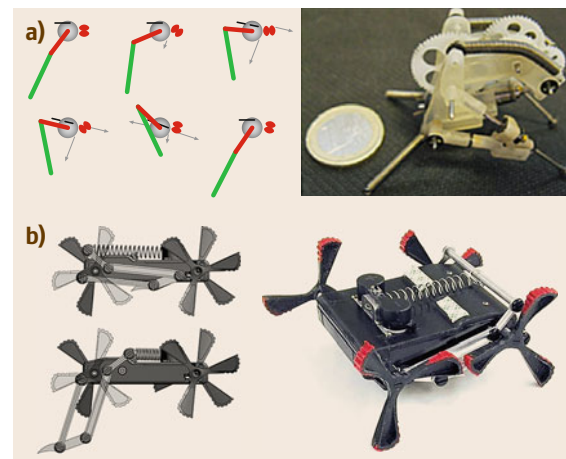


Fig.23.17a,b Toothless gear mechanism (a) Grillo (Ver.2) (after [23.92]), (b) Mini-Whig (after [23.93])

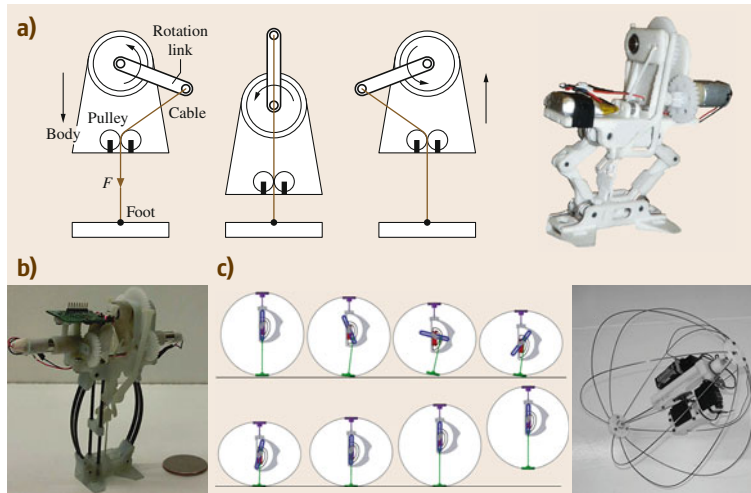


Fig. 23.18a–c Other escapement mechanism (a) MSU Jumper (after [23.94]), (b) MSU Jump-runner (after [23.95]), (c) Jollbot (after [23.96])

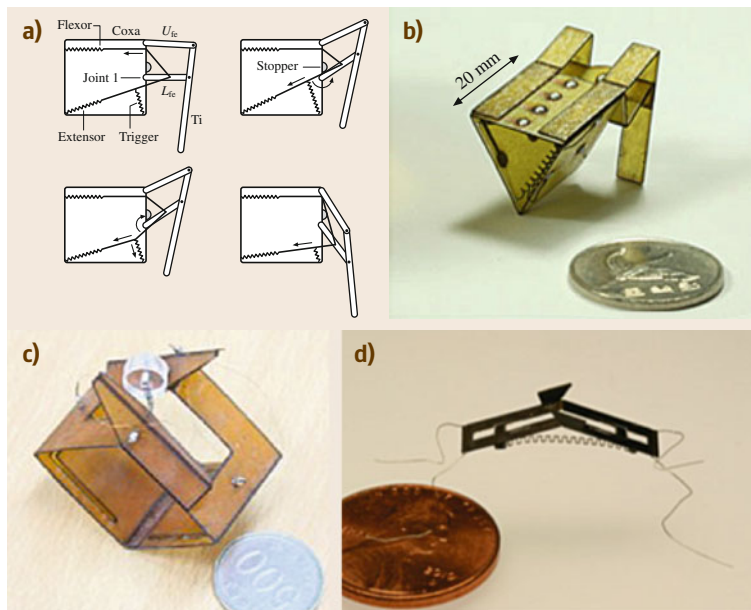


Fig. 23.19 (a) Torque-reversal mechanism, (b) Flea-inspired catapult mechanism (after [23.97]), (c) Simplified flea-inspired catapult mechanism (after [23.98]), (d) Jumping robotic insect (after [23.99])

transmission passes the toothless gear part, the transmission returns to the initial position and the stored energy is released instantly. Examples of robots using toothless gear mechanisms include Mini-Whigs [23.93] and Grillo (Ver.2) [23.92] (Fig. 23.17).

These two click mechanisms, the escapement cam mechanism and the toothless gear mechanism, are commonly used for jumping mechanisms, but other methods have also been developed (Fig. 23.18 and [VIDEO 280](#)). The catapult mechanism of MSU Jumper [23.94] and MSU Jump-Runner [23.95] is similar to the escapement cam mechanism, except for the absence of a cam. Instead of using a cam, it uses a one-way bearing. This mechanism can be separated in two

parts based on the critical point in the jump cycle. Before passing the critical point, the one-way bearing cannot rotate freely, so it rotates to the direction of energy storage. On the other hand, after passing that point, it can rotate freely and release the stored energy for jumping. The catapult mechanism in Jollbot [23.96] is similar to the mechanism in the MSU Jumper. Its structure's slit acts like a one-way bearing.

A flea-inspired catapult mechanism [23.97] is different from aforementioned catapult mechanisms (Fig. 23.19 and [VIDEO 281](#)). It consists of three SMA coil springs: (1) Flexor, (2) Extensor, and (3) Trigger. The SMA is activated by heat induced from applied current. The flea catapult mechanism begins by activating

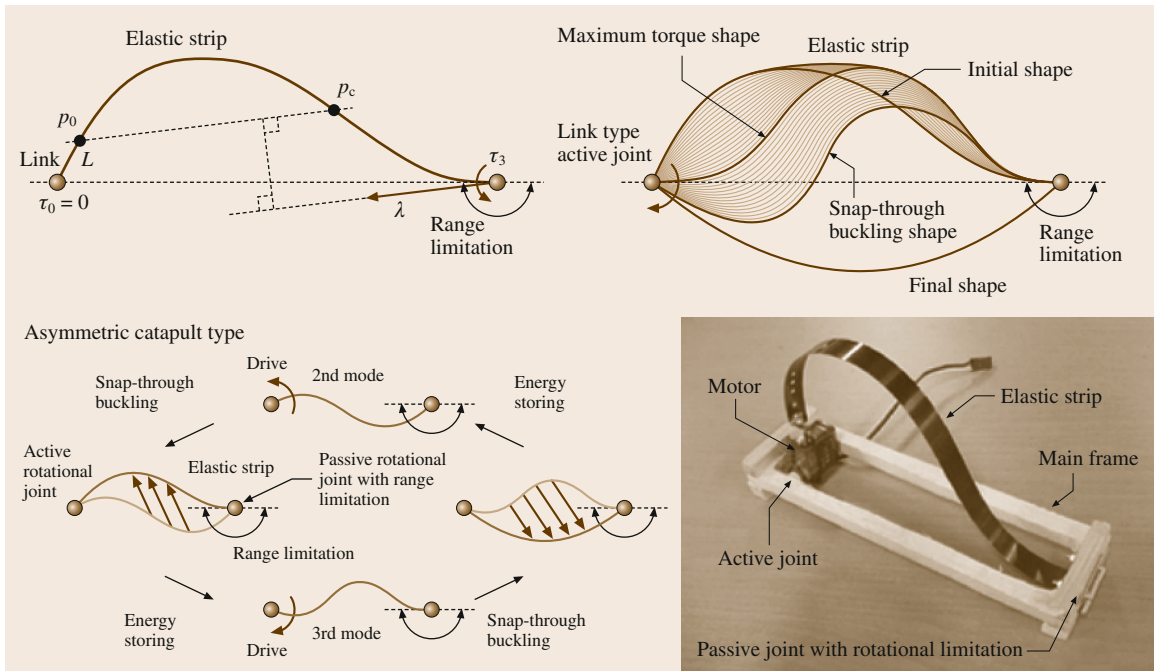


Fig. 23.20 An asymmetric robotic catapult jumping robot (after [23.100])

the flexor that folds the leg. Then, the extensor is activated. Because the direction of the torque generated by the extensor force is in the folding direction, the leg does not move and energy is stored in the extensor SMA coil spring. After energy is storage, activation of the trigger attached to the extensor pulls the extensor until it passes the joint. As a result, the direction of the torque generated by the extensor is reversed and the robot starts to jump. This mechanism uses muscle-like actuators to create the torque reversal mechanism, which enables simple design. Variation of the torque reversal mechanisms have been developed with lesser number of actuators but maintaining the same biological principle: the simplified flea-inspired catapult mechanism [23.98] and the jumping robotic insect [23.99].

An asymmetric robotic catapult jumping robot [23.100] also has a unique catapult mechanism (Fig. 23.20). It utilizes buckling in a compliant beam to jump. It consists of a main frame, an elastic strip and a motor. The elastic strip is connected to the main frame with a free rotational joint that can rotate from 0° to 180° and is connected to a motor that can control the rotation angle. When one of the elastic strip's ends is fixed to the main frame, adjusting the angle of the other end can be in a snap-through buckling shape. This can produce bidirectional jumps, but the buckling modes are different on either side.

Jumping mechanisms for microrobots [23.101] have been built using microelectromechanical systems

(MEMS) manufacturing methods to create a silicon body, silicon leg, and a series of PDMS springs (Fig. 23.21a). This mechanism consists of two rigid bodies connected by PDMS springs and is activated by an external force. The robot includes only the mechanisms required to demonstrate a jump. The actuation combined elastomer mechanism is shown in Fig. 23.21b [23.101]. It used chevron actuators. These actuators are used to linearly pull and release the PDMS spring embedded into an etched silicon structure for jumping. The mechanism's PDMS springs are designed

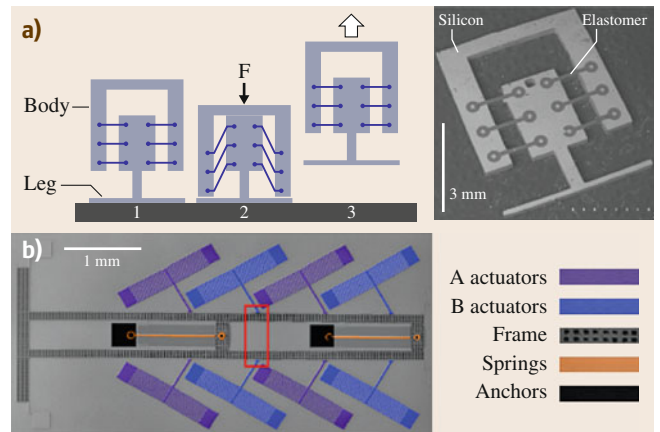


Fig. 23.21 (a) Microrobot (after [23.101]), (b) a colored SEM image of the actuated mechanism (after [23.101])

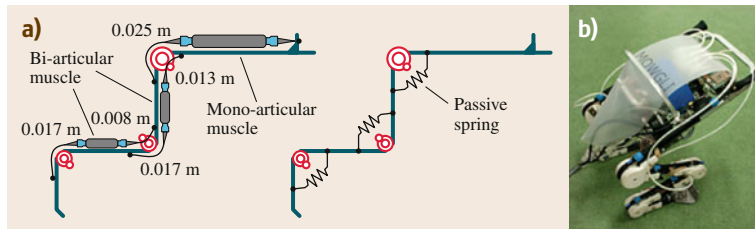


Fig. 23.22 (a) Pneumatic artificial muscles arranged like bi-articular muscle, (b) Mowgli (after [23.102])

to be similar to resilin – the elastomer that appears in insects [23.101].

In large-scale jumping, to overcome muscle's limited speed, large animals use their long legs or special arrangements of muscles and bones such as *bi-articular muscles*. They are muscles that work on two joints. In a mechanical linkage that is composed of bi-articular muscle and bones, the two joints affect each other. During the jumping process, these conditions can be helpful for generating the optimum force. The large jumping robot *Mowgli* uses long legs and pneumatic artificial muscles that are arranged like bi-articular muscle and it can be seen in Fig. 23.22 and in [VIDEO 285](#) [23.102].

Specifications of the jumping robots are summarized in Table 23.1.

23.3.8 Gripping and Perching

In nature, insects and animals climb various kinds of terrains – from flat and smooth to wavy and rugged surfaces. Some animals evolved in a way that passively adapts to unstructured environments to reduce the energy consumption and control complexity. From the view point of robotics, these properties have the potential to increase energy efficiency and reduce system complexity. Therefore, many researchers have employed such mechanism to gripping and perching devices.

Hawkes et al. developed a mechanism that allows large patches of directional dry adhesives to conform to the topology of the surfaces they are in contact with [23.103]. The mechanism uses a rigid tile supported by a compliant material loaded by an inextensible tendon – inspired by the tendon system and the fluid-filled sinus in gecko toes. This mechanism permits the adhesive to make full contact with the surface and have uniform loading despite significant errors in alignment. *Hawkes et al.* also developed a gasper for landing of microair vehicles and grappling objects in space using gecko-inspired directional adhesives, as shown in [VIDEO 413](#) [23.104] (Fig. 23.23).

There are several devices and robots that employ microspines for grasping rough surfaces easily seen in nature. *Kim et al.* proposed arrays of miniature spines that catch opportunistically on surface asperities [23.55]. *Desbiens et al.* proposed a small and unmanned aircraft that can land, perch and take off from vertical surfaces, as shown in [VIDEO 412](#) [23.105] inspired by squirrels that reduce their horizontal velocity up to 60% prior to impact to distribute impact over all four limbs. *Spenko et al.* developed a hexapedal climbing robot using rows of toes having microspine [23.56]. *Parness et al.* also employed 16 carriages, each of which contains 16 microspines that conform to mm-scale and below, as shown in [VIDEO 414](#) [23.106] (Fig. 23.24).

Trimmer et al. employed a passive gripping method found in caterpillars [23.107]. Caterpillars use their re-

Table 23.1 Specifications of the jumping robots

Robot	Actuator	Length	Weight	Jumping height	Initial velocity
7 g jumping robot [23.87]	Motor	5 cm	7 g	1.4 m	5.9 m/s
Grillo(Ver.1) [23.86]	Motor	5 cm	15 g	–	1.5 m/s
Grillo(Ver.2) [23.92]	Motor	3 cm	10 g	–	3.6 m/s
Mini-Wheg [23.93]	Motor	9–10 cm	90–190 g	0.18 m	–
MSU Jumper [23.94]	Motor	6.5 cm	23.5 g	0.87 m	–
MSU Jump-runner [23.95]	Motor	9 cm	25 g	1.43 m	–
Jollbot [23.96]	Motor	30 cm	465 g	0.218 m	–
Flea-inspired catapult mechanism [23.97]	SMA	2 cm	1.1 g	0.64 m	4.4 m/s
Simplified flea-inspired jumping mechanism [23.98]	SMA	3 cm	2.3 g	1.2 m	7 m/s
Jumping robotic insect [23.99]	SMA	2 cm	0.034 g	0.3 m	2.7 m/s
An asymmetric robotic catapult jumping robot [23.100]	Motor	17 cm	30 g	0.2 m	–
Microrobot [23.101]	None	0.4 cm	0.008 g	0.32 m	3 m/s
Mowgli [23.102]	Pneumatic	1 m	3 kg	0.4 m	–

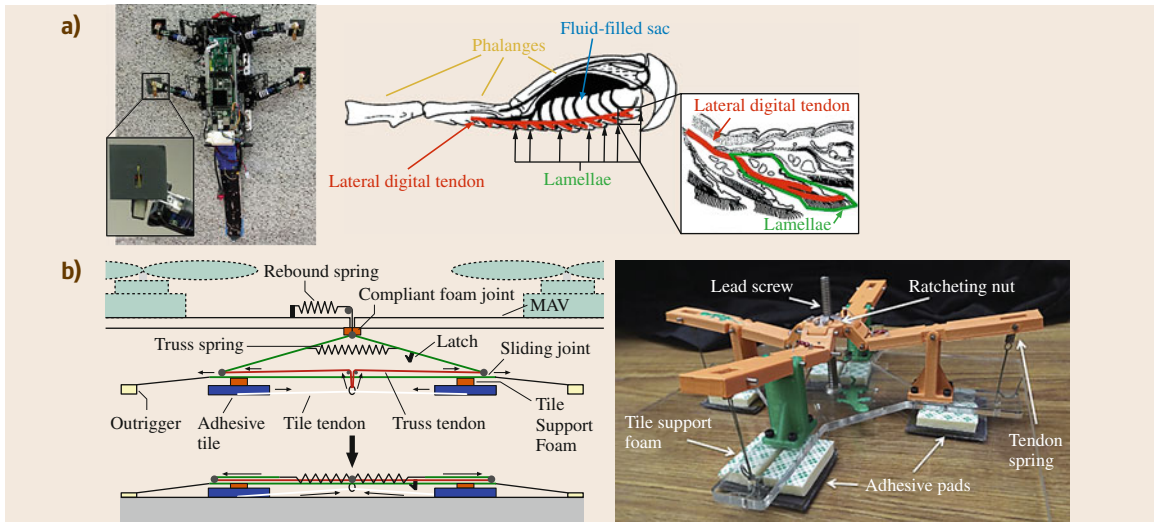


Fig.23.23a,b Graspers based on Gecko-inspired adhesives. (a) Gecko-inspired toe used in RiSE robot (left) and cross section of the gecko foot (right) (after [23.103]), (b) Collapsing truss grasper (left) and pivot linkage grasper (right) (after [23.104])

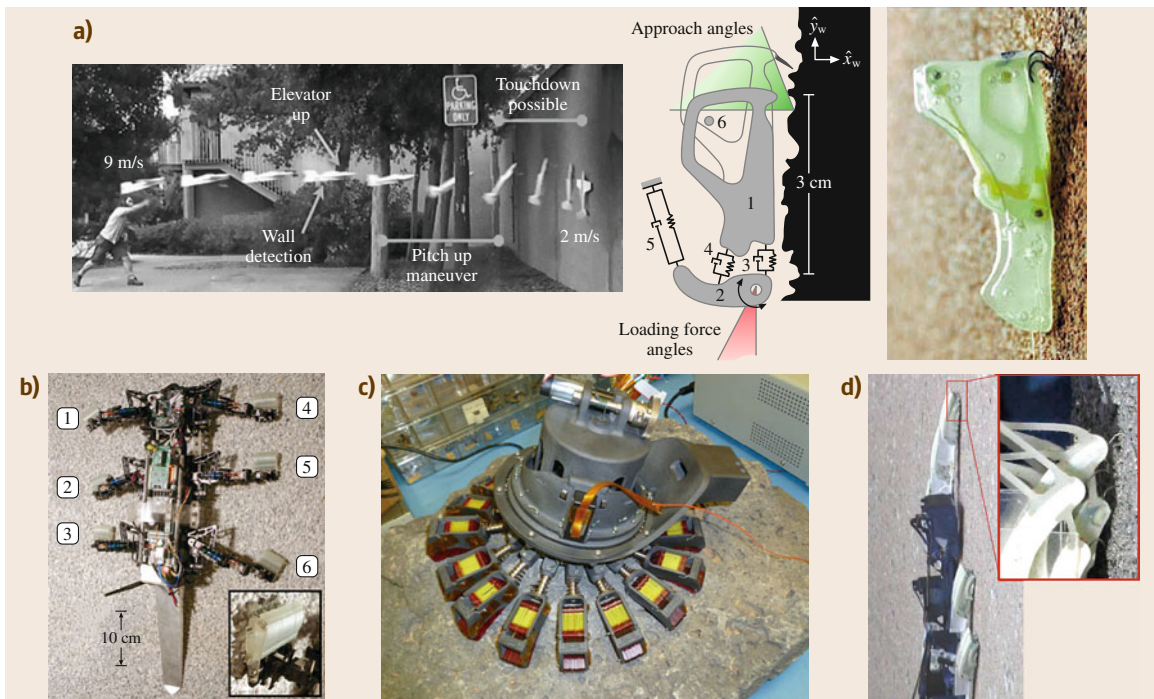


Fig.23.24a-d Microspine-based robots. (a) Landing and perching UAV (after [23.105]), (b) RiSE robot (after [23.56]), (c) sample acquisition tool (after [23.106]), (d) Spinybot (after [23.55])

tractor muscles to release the grip, which means that they do not consume any energy during gripping. Like the caterpillar, Trimmer et al. designed the grippers so that gripping is released when the SMA spring actuator is activated. Jung et al. proposed an underactuated

mechanism based on flexural buckling [23.108]. The flexural buckling mechanism is inspired by the soft cuticle of a caterpillar's feet, which largely deforms depending on the shape of the contacting surface. The large deformation in the engineered device, flexural

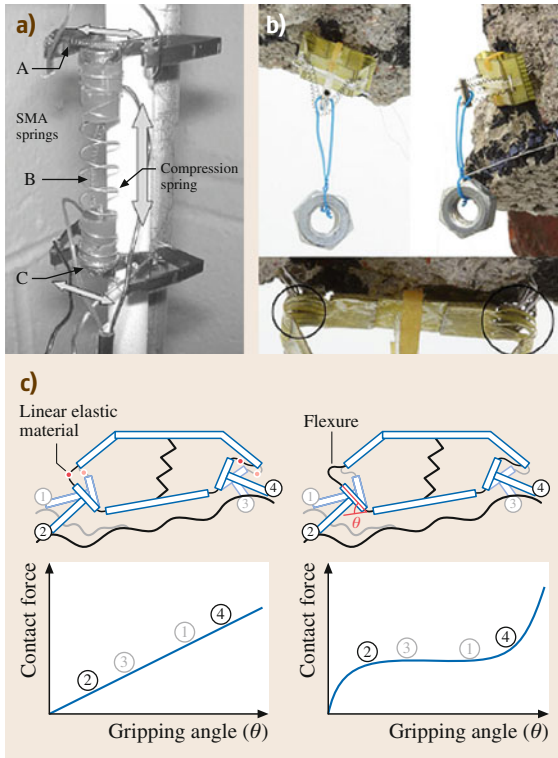


Fig. 23.25 (a) Passive gripping system (after [23.107]), (b) caterpillar-inspired underactuated gripper and (c) constant force region by flexural buckling (after [23.108]) ◀

easily be scaled up or down depending on required scale. [VIDEO 409](#) shows the small and large scale gripper that can achieve adaptive grasping (Fig. 23.25).

The octopus performs crawling movements with the same limbs used for grasping and manipulation, as shown in [VIDEO 411](#). Calisti et al. proposed an octopus-inspired solution for movement and manipulation [23.109]. To implement octopus-like motion, they employed a steel cable for elongating and shortening and fiber cables for bending, which is inspired by the longitudinal muscles found in an octopus shown in Fig. 23.26.

Kim et al. developed flytrap-inspired high-speed gripper, as shown in [VIDEO 410](#) [23.110]. Flytraps achieve fast capturing by using the bistable structural characteristic of its leaf. To achieve similar bistability, Kim et al. used asymmetrically laminated carbon fiber reinforced preregs (CFRP). They also utilized a deformable surface having kinematic constraints, which constrain the curvature of the artificial leaf. Therefore, the curved leaf can be actuated by bending the straight edge orthogonal to the curve, a process called bending propagation.

buckling with an adequately selected length, provides wide gripping range with a narrow range of force variation. This provides a sufficient number of contacts with even contact forces, enabling adaptive gripping on various surfaces. In addition, design of the gripper can

Doyle et al. developed an avian-inspired passive perching mechanism for quadrotors for perch-and-stare, as shown in [VIDEO 415](#) [23.111]. Songbirds had evolved to sleep while perching. When they perch on a branch, the tendon connected from the ankle and

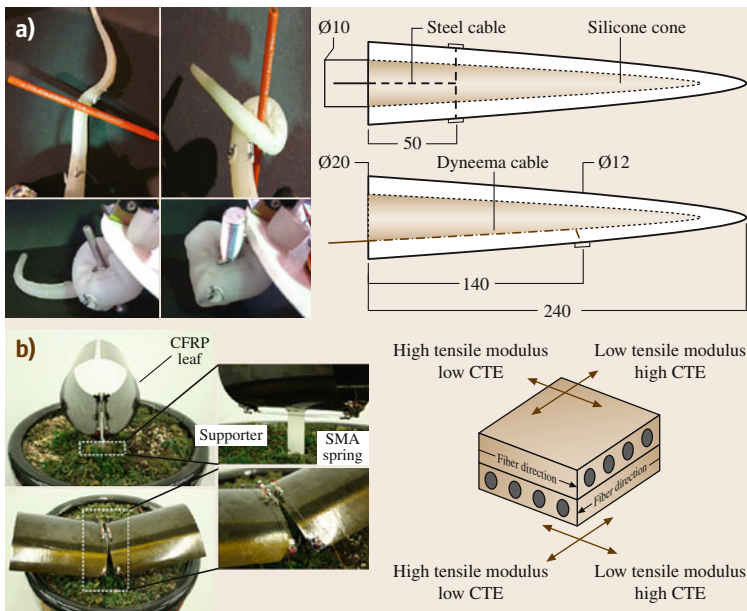


Fig. 23.26 (a) Octopus-inspired manipulation (left) and tendon-driven mechanism (right) (after [23.109]), (b) Flytrap-inspired gripper and Orthogonally laminated CFRP (right) (after [23.110])

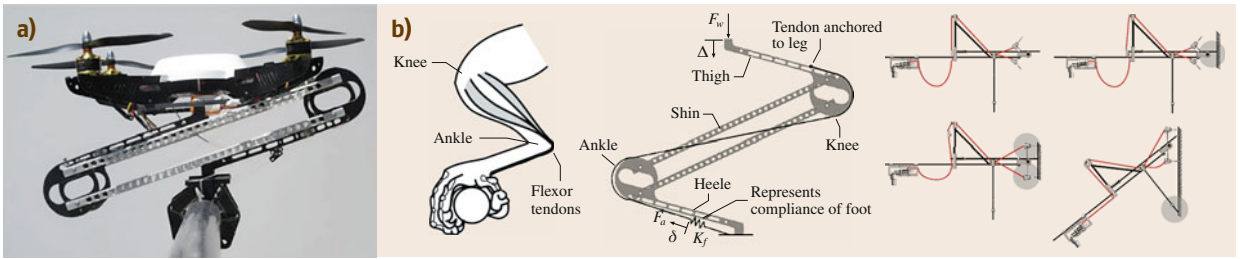


Fig. 23.27 (a) Avian-inspired perching mechanism with UAV (left) anatomy and mechanism design (right) (after [23.111]), (b) perching mechanism and process (after [23.112])

the rear side of toe automatically cause the toe to grip the branch. This allows the songbirds to tightly grip the branch without any muscular effort. Inspired by this, Doyle et al. used a four-bar mechanism and a tendon connected from the knee to the ankle and foot to couple landing motion with grasping. Kovač et al. presented

a 4.6 g perching mechanism for microaerial vehicles (MAVs) to make them perch on various walls such as tree and concrete buildings [23.112], as shown in [VIDEO 416](#). To achieve high impact force, the needles snap through as the trigger collides with the target surface (Fig. 23.27).

23.4 Material and Fabrication

23.4.1 Shape Deposition Manufacturing

The fundamental concept of shape deposition manufacturing (SDM) is layered molding manufacturing with CNC machining process. It not only create complex 3-D shapes rapidly, but also enables high precision finishing and large design flexibility. This concept is initially proposed by Weiss et al. [23.113]. Figure 23.28a shows the steps of the SDM process and Fig. 23.28b shows fabrication result [23.114]. After depositing support material, the support was fabricated by CNC machining to make high precision surface. Li et al. shows

that it is possible to embed a various functional material such as sensors to the structure [23.115] and Marra et al. show that this process can be used in the fabrication of scaffolds for bone tissue engineering [23.116].

In 1999, the SDM process was first used for robot design by Bailey et al. [23.114]. Robot design methods based on the SDM process have advantages that it does not need complex assembly or connecting methods, and it can embed sensors and actuators directly into the body structure. In other words, the structure is build and assembled at the same time, and this

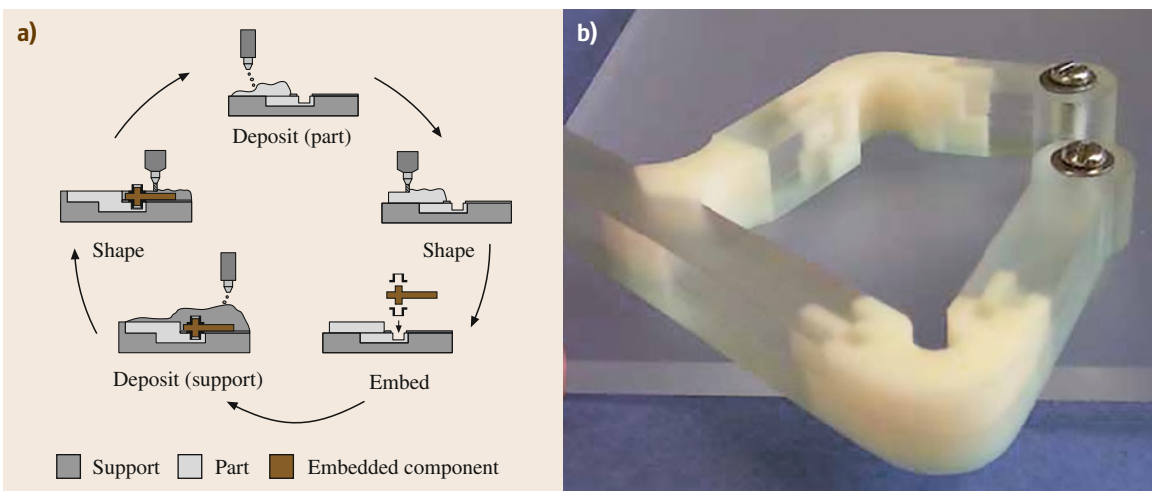


Fig.23.28a,b Shape deposition manufacturing (a) Process, (b) result of SDM process for robot mechanism design (after [23.114])

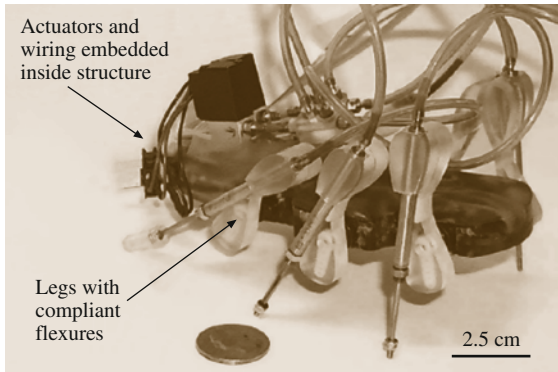


Fig. 23.29 Hexapedal robot built by SDM process (after [23.117])

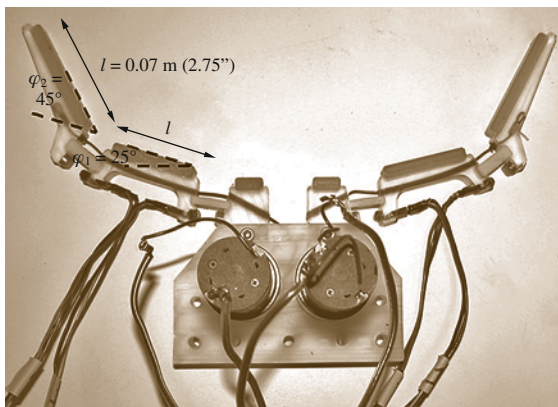


Fig. 23.30 Robotic gripper built by SDM process (after [23.118])

characteristic leads to enhanced manufacturability in small-scale applications. To build a desired mechanism, the author used multiple cycles of material deposition and shaping as shown in Fig. 23.28a. Multiple materials were used in fabrication to create variable characteristic to each functional part. More flexible material was used for joints and rigid material was used for links. The flexible components are not only used as articulated joints, but also as dampers and springs to control the impedance of a mechanism. *Binard et al.* suggested a design framework for the SDM

process for mechanism design, making more multifarious applications possible [23.119]. Figure 23.29 shows *Sprawlita*, a hexapedal robot fabricated based on the SDM process. Using the SDM process, actuators and wires are embedded in the body structure, resulting in robust performance and minimal manual assembly operations [23.117]. Robotic grippers can also be made by the SDM process (Fig. 23.30) [23.118]. All of joints, links, and sheath for the actuating wire were fabricated and assembled simultaneously. Embedded sensors are also possible. Force sensors embedded in the fingertips of a robotic SDM gripper have been demonstrated [23.120]. Using a soft base material for the robot, it is also possible to design a human-friendly SDM robot [23.121].

23.4.2 Smart Composite Microstructures

In the late 1990s, researchers at the University of California, Berkeley began a project to create a robotic insect capable of sustained autonomous flight – the micromechanical flying insect was born [23.122]. Among the many challenges for this project, how to manufacture and what materials should be used for structures, mechanisms, and actuators were primary concerns. Recognizing the lack of a viable *meso-scale* manufacturing method, the team lead by Fearing attempted multiple techniques including folded triangular stainless steel beams [23.123] and eventually settled on multilayer composites [23.124]. In this paradigm, later called smart composite microstructures (SCM) [23.50], layers of materials are machined, aligned, and laminated to form a quasi-two-dimensional (quasi-2-D) laminate. The choice of materials, 2-D layer geometries, and order of the layup allows the user to create an array of rigid components separated by compliant flexures. This composite laminate, later called a *standard linkage layer* can then be folded into 3-D shapes and mechanisms.

The SCM process presents a new paradigm of design and fabrication for developing small-scale robots. Planar fiber-reinforced prepreg (FRP) and flexure hinges replace conventional links and joints in the robot mechanism. The composite laminating process is

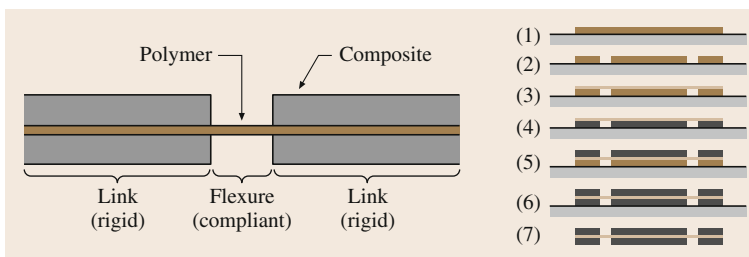


Fig. 23.31 Schematic illustration of a single joint unit in SCM and the layup of laminating process (after [23.50])

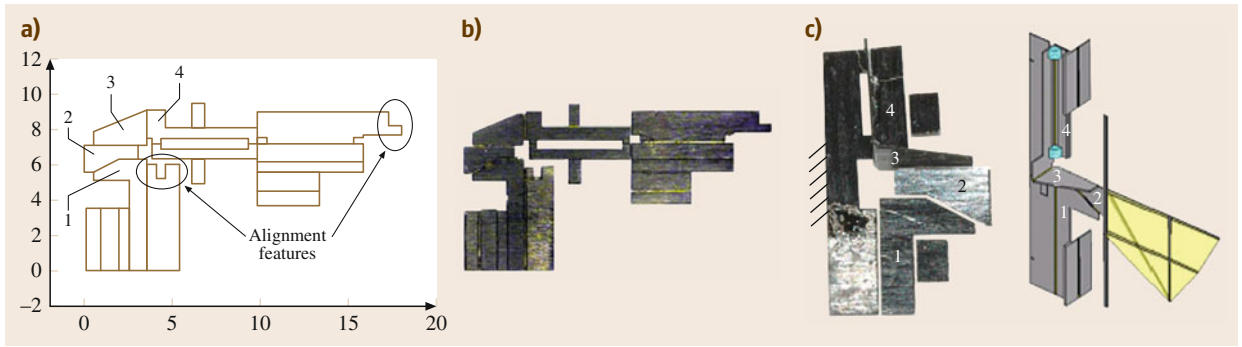


Fig.23.32a–c Spherical five-bar linkage structure created by the SCM fabrication process (after [23.52]). (a) The pattern design of a rigid face sheet, (b) laser-cut and cured microcomposite sheet before folding, (c) SCM spherical five-bar linkage for transmission of MFI

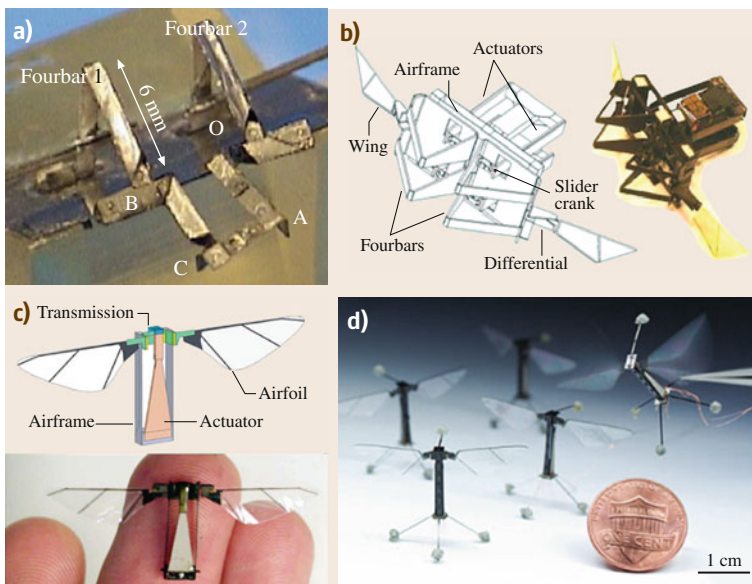


Fig.23.33a–d Various generations of MFI. (a) Wing transmission made of steel face sheet (after [23.123]). (b) Thorax mechanism with five-bar spherical linkage SCM (after [23.124]). (c) The Harvard robotic fly is capable of flapping-wing liftoff (after [23.50]). (d) The Harvard robotic fly is the first robotic insect capable of unconstrained controlled flight (after [23.125])

adopted instead of conventional machining and assembly processes which are difficult to apply to building a small-scale robot mechanism. Figure 23.31 shows a single unit of the links and the flexure hinge joints which are the key building blocks of the SCM process [23.50]. The flexure joint is a polymer film that can be bent easily and eliminating friction losses that are the dominant cause of reduced efficiency in small-scale robot mechanisms.

Rigid face sheets of fiber-reinforced composites sandwich polymers and joints are created at the gap between face sheets. The resulting quasi-2-D sheets are then folded into 3-D structures. The face sheets of rigid composite materials are carefully patterned to create robot mechanisms. For example, Fig. 23.32a is a 2-D pattern designed for creating a spherical five-bar linkages as shown in Fig. 23.32c. This is the wing

transmission linkage in the early versions of micromechanical flying insect (MFI) [23.52].

Figure 23.33 shows the various versions of the MFI developed using the SCM fabrication process. Figure 23.33a is the early version of a transmission that uses a steel face sheet [23.123]. Figure 23.33b is the next generation of the MFI fabricated using a carbon fiber composite (CF) sheet and polyester film. It has 26 joints, 4-DOF, four actuators, and two wings. CF composites materials improve the performance of MFI thorax structure by reducing the inertia by a factor of three and increasing the resonant frequency by 20% [23.124]. A later version with a 3-DOF transmission (two passive DOF) and a single bimorph PZT actuator as shown in Fig. 23.33c was able to produce sufficient thrust to achieve liftoff [23.52]. Passive dynamics in the thorax structures simpli-

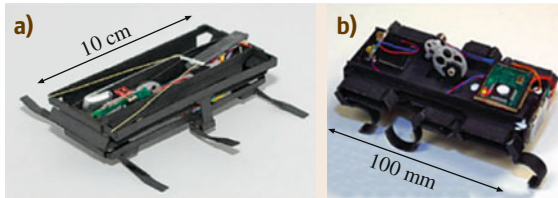


Fig. 23.34 DASH (after [23.8])

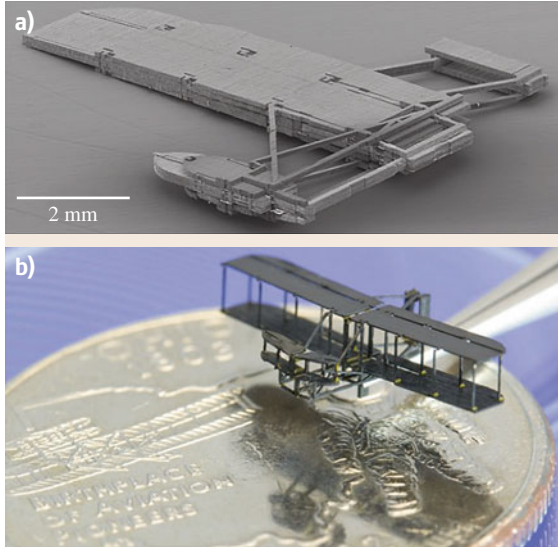


Fig. 23.35a,b 1:900 scale 1903 Wright Flyer model 14 mm in wing span (after [23.126]). After laminating layout (a), model after folding (b)

fies the design and reduces undesired coupling between the degrees of freedom. Controlled flight is accomplished by separated actuator design shown in Fig. 23.33d. Tethered but unconstrained stable hovering and basic controlled manoeuvres are demonstrated [23.125].

The SCM fabrication process can be extended to larger scales by using various sheet materials. Figure 23.34 shows centimetre scale crawling robots that are built using the SCM fabrication process with cardboard and adhesive films in place of the composites used in the MFI. This new paradigm is fast and inexpensive – both in the materials used and the required infrastructure. Furthermore, novel bio-inspired robot mechanism that produce high performance can be created easily as shown in Fig. 23.34. Figure 23.34a is a small, lightweight, power autonomous running robot, DASH [23.8]. It is capable of running at speeds up to 15 body lengths per second and surviving falls from large heights, due to the unique compliant nature of its structures. The design can be modified easily and achieve high performance with regard to stability, speed, and maneuverability as shown in Fig. 23.34b [23.10].

23.4.3 Pop-Up Book MEMS

In order to streamline the development of high performance and economical robots, many assembly tools have been developed to assist with robot construction at various scales. However, in millimetre-scale robots, many challenges arise in the fabrication process and handling many individual parts for assembly. Pop-up books and paper folding inspire the solution for eliminating the onerous assembly process with small individual parts in the fabrication process of the millimetre-scale robotic structures. Monolithic fabrication using pop-up book-inspired designs enables efficient batch processing starting from multiple layered composites similar to the basic elements used in SCM. The carefully designed layers are interconnected and allow folding mechanisms of high complexity. Once folding ensues, the complex 3-D structures are created by parallel mechanisms created in the thickness

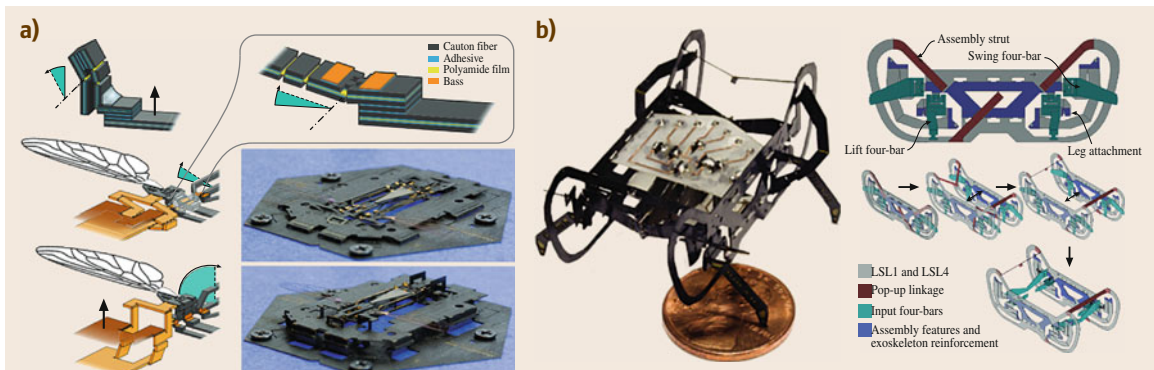


Fig. 23.36 (a) Mobee, monolithic design of MFI [23.127], (b) HAMR-VP, a 1.27 g quadrupedal microrobot manufactured using the PC-MEMS and pop-up assembly techniques (after [23.16])

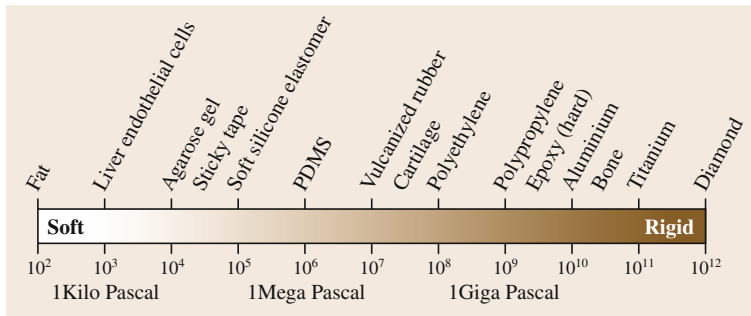


Fig. 23.37 Young's modulus for various materials (after [23.128] which was also adapted by Autumn et al. in [23.63])

of the laminate. Figure 23.35 presents a pop-up structure of 1:900 scale 1903 Wright Flyer model, 14 mm in wing span [23.126]. The model consists of six rigid CF composite layers, seven adhesive layers, and two polymer flexure layers. Multiple rigid-flex folding layers are stacked and selectively bonded. The idea is previously applied to microelectric mechanical systems (MEMS) process. Combining this idea and pop-up book designs, the fabrication process is developed for building micro robotic systems including robot structures and actuators.

Figure 23.36 shows two examples that are designed and fabricated by the pop-up book MEMS process. Figure 23.36a is the Mobee (Harvard robotic fly using the monolithic pop-up book MEMS design methods) [23.127]. In [VIDEO 398](#), it demonstrates how the pop-up book MEMS process enables mass production by parallel manufacturing on a single sheet and reduces entire fabrication time by eliminating onerous assembly tasks. Figure 23.36b is a small-scale quadruped crawling robot designed by pop-up book MEMS techniques. This device demonstrates how complex millimeter-scale robot structures are capable of pop-up assembly [23.16]. Twenty-three material layers are cut by precision laser machining and laminated with selective adhesion. After popup, the body frame is created and other components such as a circuit board and actuators are bonded on the frame.

23.4.4 Other Fabrication Methods

In nature, animals use soft parts of their body for generating locomotion, morphing configuration, and adapting to the environment. In order to maximize the utility of their compliance, some bio-inspired robots are primarily composed of soft materials such as fluids, gels, granules, and soft polymers. With respect to compliance, soft materials vary with a wide range of elastic (Young's) modulus [23.128] (Fig. 23.37). Therefore, bio-inspired robots should be built by different fabrication methods depending on their constituent materials.

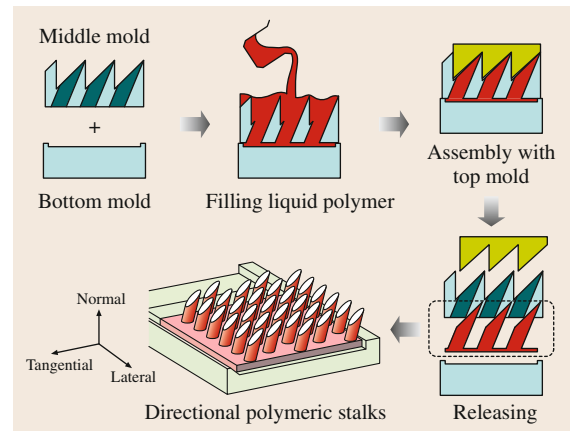


Fig. 23.38 Manufacturing process of directional adhesion pad (after [23.58])

Soft Lithography

Soft lithography was originally proposed for micro- and nanostructure manufacturing in 1998 [23.129]. Early soft lithography used an elastomeric stamp with patterned relief structures on its surface to generate desired patterns and structures. In bio-inspired robotics, for example, a directional adhesion pad inspired by a gecko foot's microscale adhesion spines was developed by a similar fabrication method to soft lithography [23.58] (Fig. 23.38).

Advances of convenient, effective and low-cost soft lithography allowed it to be utilized not only in the micro and nano scale in bio-chemical fields, but also in macro-scale robotics. Moreover, development and popularization of additive manufacturing process using 3-D printers which can design molds with various shapes easily and rapidly have helped soft lithography to be applied in robotics. Soft lithography has become a representative manufacturing method for bio-inspired soft robots since soft lithography was first applied to manufacturing bio-inspired soft robots [23.130–133] (Fig. 23.39). In soft lithography for bio-inspired soft robots, uncured elastomeric polymers, such as PDMS or EcoFlex, are poured into a mold designed with

configuration of the structure. After curing, the soft materials form a structure containing multiple air chambers and pneumatic channels. Such kind of structure is so-called a pneumatic network (PneuNet) or bending fluidic actuator (BFA).

This structure allows the robots to generate sophisticated locomotion such as gripping, walking, and crawling as shown in Fig. 23.40. In addition, extra embedded channels can control the flow of a dyeing solution so that a soft robot can camouflage by changing body color to match the color of the surroundings [23.135]. The actuation or locomotion of robots manufactured by soft lithography depends on the elastic modulus of materials and the geometry and position of air chambers [23.136].

Furthermore, soft lithography in robotics has advanced by mixing different kind of materials. By embedding sheets or fibers into elastomers, an actuator has asymmetric compliance which allows the structure to be flexible but not extensible, so that the actuator can generate a wide range of motions such as bending, extension, contraction, twisting, and others [23.137] (Fig. 23.41). By embedding magnets into elastomers, a soft robot can attach, detach, and easily align modules that have a unique function per each module depending on the task [23.138].

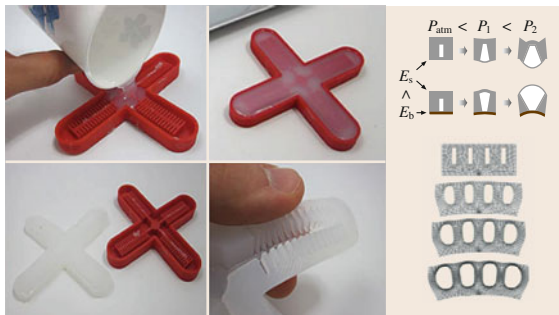


Fig. 23.39 Soft lithography of pneumatic network (PneuNet) or bending fluidic actuator (BFA) (after [23.130, 133, 134])



Fig. 23.40 Bio-inspired soft robots and actuators manufactured by soft lithography (after [23.130, 131, 135, 136])

To overcome a slow actuation, which is a typical issue for soft robots, the design of segmented air chambers divided by slits was introduced as an alternative soft actuator [23.139]. As a result, a fast PneuNet structure had high rate of actuation, improved 25 times relative to the slow PneuNet actuators. Also, a reduced change of volume minimizes fatiguing the materials, and thus the durability improves to a level that the actuator does not fail within a million cycles of full bending.

Actuator Embedded Molding

Bio-inspired soft robots potentially have infinite degrees of freedom and the nonlinearity of soft materials creates difficulty in generating desired postures and motion. Actuator-embedded molding is commonly used to manufacture the soft structure for bio-inspired robots. In actuator-embedded molding, the design considerations are the type of the actuator and the actuator's location and direction in the soft structure. For an example of a bio-inspired robot using actuator-embedded molding, a turtle-like swimming robot was created using a smart soft composite (SSC) structure to create bending and twisting deformation [23.77] (Fig. 23.42). The SSC structure consists of an actuator-embedded layer as an active component, a patterned layer as a passive component, and a soft matrix as the body as shown in Fig. 23.42. The angle of the patterned layer determines the bending direction passively, and the actuator-embedded layer generates deformation. The soft matrix helps to deform the structure continuously. Widely used

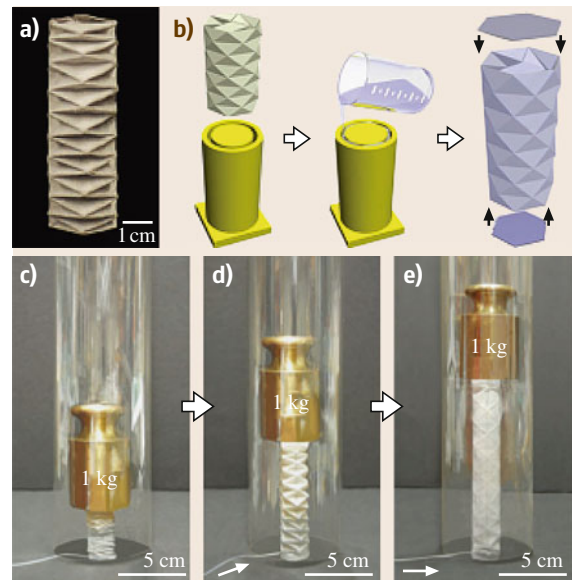


Fig. 23.41a–e Programmable paper–elastomer composites-based pneumatic actuators by using soft lithography (after [23.137])

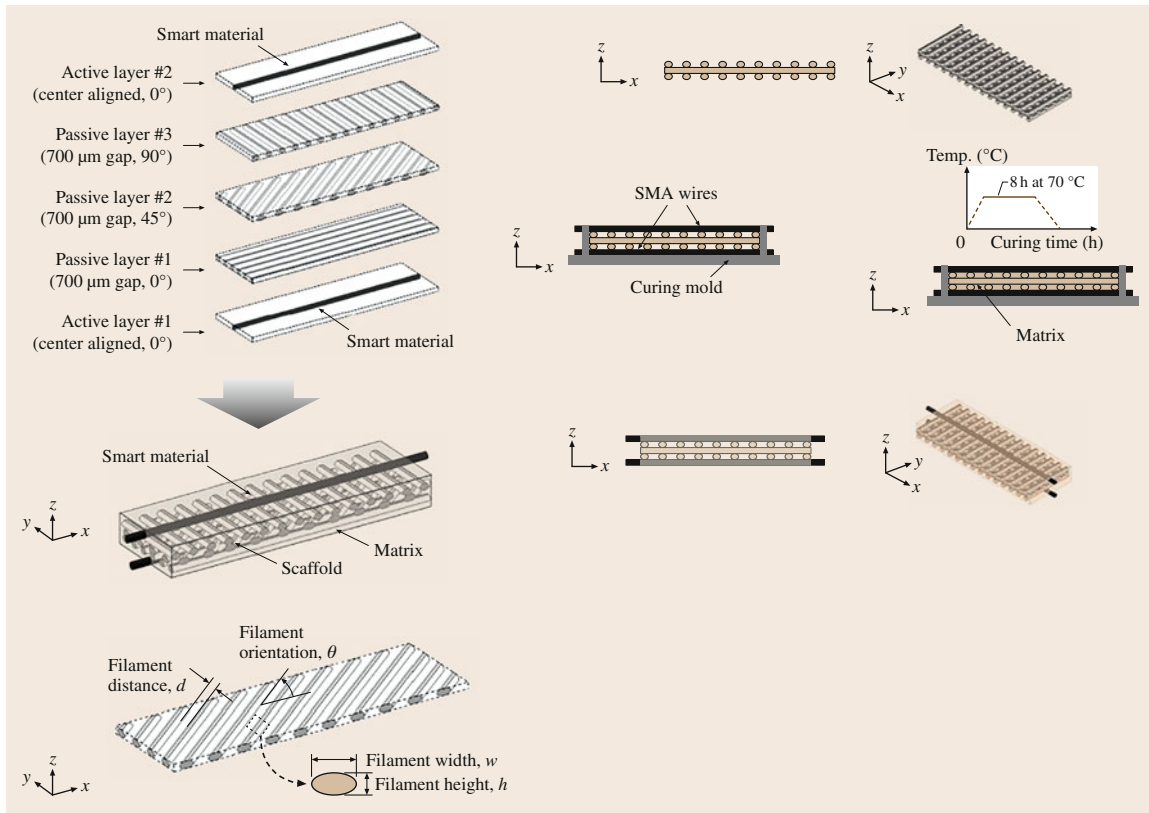


Fig. 23.42 Actuator-embedded molding for the SSC structure actuator (after [23.77])

actuators in the actuator embedded molding are wires including common wires connected with servo motors and shape memory alloys (SMA) [23.25, 77, 140].

Additive Manufacturing

Additive manufacturing or 3-D printing is a rapid prototyping (RP) process of manufacturing a 3-D solid structure of any configuration through sequential layering from a digital CAD model. Since the 1980s, various types of additive manufacturing have been developed: solid-based processes such as fused deposition modeling (FDM), photo curable liquid polymer-based processes such as stereolithography (SLA), and powder-based processes such as selective laser sintering (SLS).

23.5 Conclusion

Biomimetic robotics attempt to create devices that are capable of various types of effective interaction with natural environment, e.g., locomotion and manipulation, by using the principles of nature. Nature is full of

surprising types of movements that enables insects and animals to survive by escaping from danger or hunting for food. In this chapter, we have presented robots that attempt to recreate these feats by understanding the un-














Evolving the technology of 3-D printers, soft material deposition and even hybrid deposition of different materials with different stiffnesses are available. Thus, soft structures can be built at once, and products using hybrid deposition can have features of rigidity and softness at the same time. For example, a highly deformable 3-D printed soft robot was developed [23.141]. This robot body was printed by using a multimaterial printable 3-D printer (Objet Connex 500TM 3-D printer) with two materials: one is a soft rubber-like Objet TangoBlackPlusTM and another is a hard polypropylene-like Objet VeroWhitePlusTM. These two materials have different friction coefficients; thus, the robot can switch friction with the ground on its edge by bending the body.

derlying principles, deriving an engineering design, and fabricating them with novel methods. In recent years, engineers have succeeded in recreating insects and animals that show amazing capabilities such as climbing walls like a gecko, hovering like a fly and climbing trees like a snake. These robots have been developed to understand nature, and also to be used as tools for surveillance, information gathering, and rescue operations. However, many of these robots are still in the basic research phase and are not yet ready for everyday use.

The key open research issues remain in the broad areas of materials, fabrication, actuation, and power. Composites and polymers, together with novel fabrication methods, have enabled various novel biomimetic robots. Development of these new material and fabrication has been one of the key enabling technologies, and further development of these technologies will certainly contribute to more mature biomimetic robots. Actuation and power still remain the bottleneck of many biomimetic robots. DC motors are the actuators of choice for many biomimetic robots, and with novel transmission design, DC motors can create motions required by the robots. However, DC motors are inefficient for small-scale biomimetic robots. Although artificial muscle actuators that are based on

shrinkage or expansion of material, e.g., shape memory alloys, IPMC, electro-active polymers and shape memory polymers, promise to give robots capabilities similar to creatures that use biological muscles even at small scales. However, many issues related to robustness, efficiency, and power limit the capabilities of robots that use these actuators. Limitations of these actuators should be carefully considered to match the desired application. Development of new artificial muscle actuator that can emulate biological muscles – without the drawbacks of current actuators – is needed to open up a new era for biomimetic robots. Batteries also limit the capabilities of current biomimetic robots compared to their biological counterparts in terms of size and operation time. Development of energy-harvesting technologies together with new battery chemistries and manufacturing methods will enable longer operation time, which will contribute to realizing wider applications for biomimetic robots. Overall, biomimetic robot design is one of the most challenging areas of robot design since it requires development of various technologies to mimic the structure and function of natural systems. Therefore, development of biomimetic robots can have broader impact in many areas of engineering and science, and should be seen as a platform for various convergent technologies.

Video-References

-  VIDEO 278 The long-jumping robot 'Grillo' available from <http://handbookofrobotics.org/view-chapter/23/videodetails/278>
-  VIDEO 279 A miniature 7 g jumping robot available from <http://handbookofrobotics.org/view-chapter/23/videodetails/279>
-  VIDEO 280 A single motor actuated miniature steerable jumping robot available from <http://handbookofrobotics.org/view-chapter/23/videodetails/280>
-  VIDEO 281 The Flea: Flea-inspired light jumping robot using elastic catapult with active storage and release mechanism available from <http://handbookofrobotics.org/view-chapter/23/videodetails/281>
-  VIDEO 285 Jumping & landing robot 'MOWGLI' available from <http://handbookofrobotics.org/view-chapter/23/videodetails/285>
-  VIDEO 286 RoACH: A 2.4 g, untethered crawling hexapod robot available from <http://handbookofrobotics.org/view-chapter/23/videodetails/286>
-  VIDEO 287 A new form of peristaltic locomotion in a robot available from <http://handbookofrobotics.org/view-chapter/23/videodetails/287>
-  VIDEO 288 Meshworm available from <http://handbookofrobotics.org/view-chapter/23/videodetails/288>
-  VIDEO 289 Treebot: Autonomous tree climbing by tactile sensing available from <http://handbookofrobotics.org/view-chapter/23/videodetails/289>
-  VIDEO 290 Omegabot : Inchworm inspired robot climbing available from <http://handbookofrobotics.org/view-chapter/23/videodetails/290>
-  VIDEO 291 GoQBot: Insanely fast robot caterpillar available from <http://handbookofrobotics.org/view-chapter/23/videodetails/291>
-  VIDEO 388 SpinybotII: Climbing hard walls with compliant microspines available from <http://handbookofrobotics.org/view-chapter/23/videodetails/388>
-  VIDEO 389 Smooth vertical surface climbing with directional adhesion available from <http://handbookofrobotics.org/view-chapter/23/videodetails/389>

-  VIDEO 390 Biologically inspired climbing with a hexapedal robot
available from <http://handbookofrobotics.org/view-chapter/23/videodetails/390>
-  VIDEO 391 CLASH: Climbing vertical loose cloth
available from <http://handbookofrobotics.org/view-chapter/23/videodetails/391>
-  VIDEO 392 Torque control strategies for snake robots
available from <http://handbookofrobotics.org/view-chapter/23/videodetails/392>
-  VIDEO 393 Snake robot climbs a tree
available from <http://handbookofrobotics.org/view-chapter/23/videodetails/393>
-  VIDEO 394 Snake robot in the water
available from <http://handbookofrobotics.org/view-chapter/23/videodetails/394>
-  VIDEO 395 Salamandra Robotica II robot walking and swimming
available from <http://handbookofrobotics.org/view-chapter/23/videodetails/395>
-  VIDEO 397 ACM-R5H
available from <http://handbookofrobotics.org/view-chapter/23/videodetails/397>
-  VIDEO 398 Pop-up fabrication of the Harvard monolithic bee (Mobee)
available from <http://handbookofrobotics.org/view-chapter/23/videodetails/398>
-  VIDEO 399 Controlled flight of a biologically-inspired, insect-scale robot
available from <http://handbookofrobotics.org/view-chapter/23/videodetails/399>
-  VIDEO 400 Rhex the parkour robot
available from <http://handbookofrobotics.org/view-chapter/23/videodetails/400>
-  VIDEO 401 Mini whegs
available from <http://handbookofrobotics.org/view-chapter/23/videodetails/401>
-  VIDEO 402 Robot dragonfly DeFly explorer flies autonomously
available from <http://handbookofrobotics.org/view-chapter/23/videodetails/402>
-  VIDEO 403 Stanford Sprawl and iSprawl
available from <http://handbookofrobotics.org/view-chapter/23/videodetails/403>
-  VIDEO 405 DASH: Resilient high-speed 16 g hexapedal robot
available from <http://handbookofrobotics.org/view-chapter/23/videodetails/405>
-  VIDEO 406 HAMR3: An autonomous 1.7 g ambulatory robot
available from <http://handbookofrobotics.org/view-chapter/23/videodetails/406>
-  VIDEO 407 Undulatory gaits in a centipede millirobot
available from <http://handbookofrobotics.org/view-chapter/23/videodetails/407>
-  VIDEO 408 VelociRoACH
available from <http://handbookofrobotics.org/view-chapter/23/videodetails/408>
-  VIDEO 409 Underactuated adaptive gripper using flexural buckling
available from <http://handbookofrobotics.org/view-chapter/23/videodetails/409>
-  VIDEO 410 Flytrap-inspired bi-stable gripper
available from <http://handbookofrobotics.org/view-chapter/23/videodetails/410>
-  VIDEO 411 An octopus-bioinspired solution to movement and manipulation for soft robots
available from <http://handbookofrobotics.org/view-chapter/23/videodetails/411>
-  VIDEO 412 Landing and perching UAV
available from <http://handbookofrobotics.org/view-chapter/23/videodetails/412>
-  VIDEO 413 Dynamic surface grasping with directional adhesion
available from <http://handbookofrobotics.org/view-chapter/23/videodetails/413>
-  VIDEO 414 Gravity-independent rock-climbing robot and a sample acquisition tool
with microspine grippers
available from <http://handbookofrobotics.org/view-chapter/23/videodetails/414>
-  VIDEO 415 Avian-inspired perching mechanism with UAV
available from <http://handbookofrobotics.org/view-chapter/23/videodetails/415>
-  VIDEO 416 A perching mechanism for micro aerial vehicles
available from <http://handbookofrobotics.org/view-chapter/23/videodetails/416>
-  VIDEO 431 G9 series robotic fish
available from <http://handbookofrobotics.org/view-chapter/23/videodetails/431>
-  VIDEO 432 Ichthus
available from <http://handbookofrobotics.org/view-chapter/23/videodetails/432>
-  VIDEO 433 Autonomous, self-contained soft robotic fish
available from <http://handbookofrobotics.org/view-chapter/23/videodetails/433>
-  VIDEO 434 Robotic Ray takes a swim
available from <http://handbookofrobotics.org/view-chapter/23/videodetails/434>

References

- 23.1 R.J. Full, K. Autumn, J. Chung, A. Ahn: Rapid negotiation of rough terrain by the death-head cockroach, *Am. Zool.* **38**(5), 81A (1998)
- 23.2 R.J. Full, M.S. Tu: Mechanics of a rapid running insect: Two-, four- and six-legged locomotion, *J. Exp. Biol.* **156**, 215–231 (1991)
- 23.3 C.P. Ellington: The novel aerodynamics of insect flight: Applications to micro-air vehicles, *J. Exp. Biol.* **202**, 3439–3448 (1999)
- 23.4 U. Saranli, M. Buehler, D.E. Koditschek: RHex: A simple and highly mobile hexapod robot, *Int. J. Robotics Res.* **20**, 616–631 (2001)
- 23.5 J.M. Morrey, B. Lambrecht, A.D. Horchler, R.E. Ritzmann, R.D. Quinn: Highly mobile and robust small quadruped robots, *Proc IEEE/RSJ Int. Conf. Intell. Robots Syst. (IROS)*, Vol. 1 (2003) pp. 82–87
- 23.6 J.E. Clark, J.G. Cham, S.A. Bailey, E.M. Froehlich, P.K. Nahata, R.J. Full, M.R. Cutkosky: Biomimetic design and fabrication of a hexapedal running robot, *Proc. IEEE Int. Conf. Robotics Autom. (ICRA)*, Vol. 4 (2001) pp. 3643–3649
- 23.7 S. Kim, J.E. Clark, M.R. Cutkosky: iSprawl: design and tuning for high-speed autonomous open-loop running, *Int. J. Robotics Res.* **25**, 903–912 (2006)
- 23.8 P. Birkmeyer, K. Peterson, R.S. Fearing: DASH: A dynamic 16g hexapedal robot, *Proc. IEEE/RSJ Int. Conf. Intell. Robots Syst. (IROS)* (2009) pp. 2683–2689
- 23.9 A.M. Hoover, E. Steltz, R.S. Fearing: RoACH: An autonomous 2.4g crawling hexapod robot, *Proc. IEEE/RSJ Int. Conf. Intell. Robots Syst. (IROS)* (2008) pp. 26–33
- 23.10 A.M. Hoover, S. Burden, X.-Y. Fu, S.S. Sastry, R.S. Fearing: Bio-inspired design and dynamic maneuverability of a minimally actuated six-legged robot, *Proc. IEEE/RAS Biomed. Robotics Biomech. (BioRob)* (2010) pp. 869–876
- 23.11 A.O. Pullin, N.J. Kohut, D. Zarrouk, R.S. Fearing: Dynamic turning of 13 cm robot comparing tail and differential drive, *Proc. IEEE Int. Conf. Robotics Autom. (ICRA)* (2012) pp. 5086–5093
- 23.12 A.T. Baisch, C. Heimlich, M. Karpelson, R.J. Wood: HAMR3: An autonomous 1.7g ambulatory robot, *Proc. IEEE/RSJ Int. Conf. Intell. Robots Syst. (IROS)* (2011) pp. 5073–5079
- 23.13 K.L. Hoffman, R.J. Wood: Turning gaits and optimal undulatory gaits for a modular centipede-inspired millirobot, *Proc. IEEE/RAS Biomed. Robotics Biomech. (BioRob)* (2012) pp. 1052–1059
- 23.14 R. Sahai, S. Avadhanula, R. Groff, E. Steltz, R. Wood, R.S. Fearing: Towards a 3g crawling robot through the integration of microrobot technologies, *Proc. IEEE Int. Conf. Robotics Autom. (ICRA)* (2006) pp. 296–302
- 23.15 J.T. Watson, R.E. Ritzmann, S.N. Zill, A.J. Pollack: Control of obstacle climbing in the cockroach, *Blaberus discoidalis*. I. Kinematics, *J. Comp. Physiol. A* **188**, 39–53 (2002)
- 23.16 A.T. Baisch, O. Ozcan, B. Goldberg, D. Ithier, R.J. Wood: High speed locomotion for a quadrupedal microrobot, *Int. J. Robotics Res.* **33**, 1063–1082 (2014)
- 23.17 D.W. Haldane, K.C. Peterson, F.L. Garcia Bermudez, R.S. Fearing: Animal-inspired design and aerodynamic stabilization of a hexapedal millirobot, *Proc. IEEE Int. Conf. Robotics Autom. (ICRA)* (2013) pp. 3279–3286
- 23.18 A.S. Boxerbaum, H.J. Chiel, R.D. Quinn: A new theory and methods for creating peristaltic motion in a robotic platform, *Proc. IEEE Int. Conf. Robotics Autom. (ICRA)* (2010) pp. 1221–1227
- 23.19 S. Seok, C.D. Onal, K.-J. Cho, R.J. Wood, D. Rus, S. Kim: Meshworm: A peristaltic soft robot with antagonistic nickel titanium coil actuators, *IEEE/ASME Trans. Mechatron.* **18**, 1–13 (2012)
- 23.20 A. Menciassi, D. Accoto, S. Gorini, P. Dario: Development of a biomimetic miniature robotic crawler, *Auton. Robotics* **21**, 155–163 (2006)
- 23.21 K. Kotay, D. Rus: The inchworm robot: A multi-functional system, *Auton. Robotics* **8**, 53–69 (2000)
- 23.22 N. Cheng, G. Ishigami, S. Hawthorne, H. Chen, M. Hansen, M. Telleria, R. Playter, K. Iagnemma: Design and analysis of a soft mobile robot composed of multiple thermally activated joints driven by a single actuator, *Proc. IEEE Int. Conf. Robotics Autom. (ICRA)* (2010) pp. 5207–5212
- 23.23 J.-S. Koh, K.-J. Cho: Omega-shaped inchworm-inspired crawling robot with large-index-and-pitch (LIP) SMA spring actuators, *IEEE/ASME Trans. Mechatron.* **18**, 419–429 (2013)
- 23.24 T.L. Lam, Y. Xu: Climbing strategy for a flexible tree climbing robot – Treebot, *IEEE Trans. Robotics* **27**, 1107–1117 (2011)
- 23.25 H.-T. Lin, G.G. Leisk, B. Trimmer: GoQBot: A caterpillar-inspired soft-bodied rolling robot, *Bioinsp. Biomimet.* **6**, 026007 (2011)
- 23.26 S. Hirose, Y. Umetani: The development of soft gripper for the versatile robot hand, *Mech. Mach. Theory* **13**, 351–359 (1978)
- 23.27 H. Ohno, S. Hirose: Design of slim slime robot and its gait of locomotion, *Proc. IEEE/RSJ Int. Conf. Intell. Robots Syst. (IROS)* (2001) pp. 707–715
- 23.28 C. Wright, A. Johnson, A. Peck, Z. McCord, A. Naak-geboren, P. Gianfortoni, M. Gonzalez-Rivero, R. Hatton, H. Choset: Design of a modular snake robot, *Proc. IEEE/RSJ Int. Conf. Intell. Robots Syst. (IROS)* (2007) pp. 2609–2614
- 23.29 H. Yamada, S. Chigisaki, M. Mori, K. Takita, K. Ogami, S. Hirose: Development of amphibious snake-like robot ACM-R5, *Proc. ISR* (2005)
- 23.30 J. Gray: The mechanism of locomotion in snakes, *J. Exp. Biol.* **23**, 101–120 (1946)
- 23.31 G.S. Miller: The motion dynamics of snakes and worms, *ACM Siggraph Comput. Graph.* **22**, 169–173 (1988)

- 23.32 Z. Bayraktaroglu: Snake-like locomotion: Experimentations with a biologically inspired wheelless snake robot, *Mech. Mach. Theory* **44**, 591–602 (2009)
- 23.33 D.L. Hu, J. Nirody, T. Scott, M.J. Shelley: The mechanics of slithering locomotion, *Proc. Natl. Acad. Sci.* **106**, 10081–10085 (2009)
- 23.34 Z. Wang, S. Ma, B. Li, Y. Wang: Experimental study of passive creeping for a snake-like robot, *Proc. IEEE/ICME Int. Conf. Complex Med. Eng. (CME)* (2011) pp. 382–387
- 23.35 J.J. Socha, T. O'Dempsey, M. LaBarbera: A 3-D kinematic analysis of gliding in a flying snake, *Chrysopelea paradisi J. Exp. Biol.* **208**, 1817–1833 (2005)
- 23.36 R.L. Hatton, H. Choset: Generating gaits for snake robots: Annealed chain fitting and keyframe wave extraction, *Auton. Robotics* **28**, 271–281 (2010)
- 23.37 K.J. Dowling: *Limbless Locomotion: Learning to Crawl with a Snake Robot* (NASA, Pittsburgh 1996)
- 23.38 S. Hirose, M. Mori: Biologically inspired snake-like robots, *IEEE Int. Conf. Robotics Biomimet. (ROBIO)* (2004) pp. 1–7
- 23.39 C. Wright, A. Buchan, B. Brown, J. Geist, M. Schwering, D. Rollinson, M. Tesch, H. Choset: Design and architecture of the unified modular snake robot, *Proc. IEEE Int. Conf. Robotics Autom. (ICRA)* (2012) pp. 4347–4354
- 23.40 K.-H. Low: *Industrial Robotics: Programming, Simulation and Applications* (InTech, Rijeka 2007)
- 23.41 A.J. Ijspeert, A. Crespi, D. Ryczko, J.M. Cabelguen: From swimming to walking with a salamander robot driven by a spinal cord model, *Science* **315**, 1416–1420 (2007)
- 23.42 R. Crespi, K. Karakasiliotis, A. Guignard, A.J. Ijspeert: 1 Salamandra robotica II: An amphibious robot to study salamander-like swimming and walking gaits, *IEEE Trans. Robotics* **29**, 308–320 (2013)
- 23.43 S. Hirose, H. Yamada: Snake-like robots [Tutorial], *IEEE Robotics Autom. Mag.* **16**, 88–98 (2009)
- 23.44 N. Kamamichi, M. Yamakita, K. Asaka, Z.-W. Luo: A snake-like swimming robot using IPMC actuator/sensor, *Proc. IEEE Int. Conf. Robotics Autom. (ICRA)* (2006) pp. 1812–1817
- 23.45 P. Liljebäck, K.Y. Pettersen, O. Stavdahl, J.T. Gravdahl: Snake robot locomotion in environments with obstacles, *IEEE/ASME Trans. Mechatron.* **17**, 1158–1169 (2012)
- 23.46 P. Liljebäck, K.Y. Pettersen, Ø. Stavdahl, J.T. Gravdahl: A review on modelling, implementation, and control of snake robots, *Robotics Auton. Syst.* **60**, 29–40 (2012)
- 23.47 M.H. Dickinson: Wing rotation and the aerodynamic basis of insect flight, *Science* **284**, 1954–1960 (1999)
- 23.48 M.H. Dickinson: How animals move: An integrative view, *Science* **288**, 100–106 (2000)
- 23.49 G.C.H.E. de Croon, K.M.E. de Clercq, R. Ruijsink, B. Remes, C. de Wagter: Design, aerodynamics, and vision-based control of the Delfly, *Int. J. Micro Air Veh.* **1**(2), 71–97 (2009)
- 23.50 R.J. Wood, S. Avadhanula, R. Sahai, E. Steltz, R.S. Fearing: Microrobot design using fiber reinforced composites, *J. Mech. Des.* **130**, 052304 (2008)
- 23.51 M. Keennon, K. Klingebiel, H. Won, A. Andriukov: Development of the nano hummingbird: A tailless flapping wing micro air vehicle, *AIAA Aerospace Sci. Meet.* (2012)
- 23.52 R.J. Wood: The first takeoff of a biologically inspired at-scale robotic insect, *IEEE Trans. Robotics* **24**, 341–347 (2008)
- 23.53 K. Peterson, P. Birkmeyer, R. Dudley, R.S. Fearing: A wing-assisted running robot and implications for avian flight evolution, *Bioinsp. Biomimet.* **6**, 046008 (2011)
- 23.54 S. Hirose, A. Nagakubo, R. Toyama: Machine that can walk and climb on floors, walls and ceilings, *Adv. Robotics ICAR '05. Proc.* (1991) pp. 753–758
- 23.55 S. Kim, A.T. Asbeck, M.R. Cutkosky, W.R. Provancher: SpinybotII: Climbing hard walls with compliant microspines, *Adv. Robotics ICAR '05. Proc.* (2005) pp. 601–606
- 23.56 M. Spenko, G.C. Haynes, J. Saunders, M.R. Cutkosky, A.A. Rizzi, R.J. Full, D.E. Koditschek: Biologically inspired climbing with a hexapedal robot, *J. Field Robotics* **25**, 223–242 (2008)
- 23.57 K. Autumn, A. Dittmore, D. Santos, M. Spenko, M. Cutkosky: Frictional adhesion: A new angle on gecko attachment, *J. Exp. Biol.* **209**, 3569–3579 (2006)
- 23.58 S. Kim, M. Spenko, S. Trujillo, B. Heyneman, D. Santos, M.R. Cutkosky: Smooth vertical surface climbing with directional adhesion, *IEEE Trans. Robotics* **24**, 65–74 (2008)
- 23.59 M. Minor, H. Dulimarta, G. Danghi, R. Mukherjee, R.L. Tummala, D. Aslam: Design, implementation, and evaluation of an under-actuated miniature biped climbing robot, *Proc. IEEE/RSJ Int. Conf. Intell. Robots Syst. (IROS)* (2000) pp. 1999–2005
- 23.60 D. Longo, G. Muscato: The Alicia 3 climbing robot: A three-module robot for automatic wall inspection, *IEEE Robotics Autom. Mag.* **13**, 42–50 (2006)
- 23.61 M. Armada, M. Prieto, T. Akinfiev, R. Fernández, P. González, E. García, H. Montes, S. Nabulsi, R. Ponticelli, J. Sarriá, J. Estremera, S. Ros, J. Grieco, G. Fernández: On the design and development of climbing and walking robots for the maritime industries, *J. Marit. Res.* **2**, 9–32 (2005)
- 23.62 G.C. Haynes, A. Khripin, G. Lynch, J. Amory, A. Saunders, A.A. Rizzi, D.E. Koditschek: Rapid pole climbing with a quadrupedal robot, *Proc. IEEE Int. Conf. Robotics Autom. (ICRA)* (2009) pp. 2767–2772
- 23.63 K. Autumn, Y.A. Liang, S.T. Hsieh, W. Zesch, W.P. Chan, T.W. Kenny, R. Fearing, R.J. Full: Adhesive force of a single gecko foot-hair, *Nature* **405**, 681–685 (2000)
- 23.64 G.A. Lynch, J.E. Clark, P.-C. Lin, D.E. Koditschek: A bioinspired dynamical vertical climbing robot, *Int. J. Robotics Res.* **31**, 974–996 (2012)

- 23.65 J. Clark, D. Goldman, P.-C. Lin, G. Lynch, T. Chen, H. Komsuoglu, R.J. Full, D. Koditschek: Design of a bio-inspired dynamical vertical climbing robot, *Robotics Sci. Syst.* (2007)
- 23.66 P. Birkmeyer, A.G. Gillies, R.S. Fearing: Dynamic climbing of near-vertical smooth surfaces, *Proc. IEEE/RSJ Int. Conf. Intell. Robots Syst. (IROS)* (2012) pp. 286–292
- 23.67 K.A. Daltorio, T.E. Wei, S.N. Gorb, R.E. Ritzmann, R.D. Quinn: Passive foot design and contact area analysis for climbing mini-whegs, *Proc. IEEE Int. Conf. Robotics Autom. (ICRA)* (2007) pp. 1274–1279
- 23.68 O. Unver, A. Uneri, A. Aydemir, M. Sitti: Geckobot: A gecko inspired climbing robot using elastomer adhesives, *Proc. IEEE Int. Conf. Robotics Autom. (ICRA)* (2006) pp. 2329–2335
- 23.69 S.A. Bailey, J.G. Cham, M.R. Cutkosky, R.J. Full: A biomimetic climbing robot based on the gecko, *J. Bionic Eng.* **3**, 115–125 (2006)
- 23.70 M.P. Murphy, C. Kute, Y. Mengüç, M. Sitti: Waalbot II: Adhesion recovery and improved performance of a climbing robot using fibrillar adhesives, *Int. J. Robotics Res.* **30**, 118–133 (2011)
- 23.71 D.S. Barrett: Propulsive Efficiency of a Flexible Hull Underwater Vehicle, Ph.D. Thesis (MIT, Cambridge 1996)
- 23.72 J. Liu, H. Hu: Biological inspiration: From carangiform fish to multi-joint robotic fish, *J. Bionic Eng.* **7**, 35–48 (2010)
- 23.73 G.-H. Yang, K.-S. Kim, S.-H. Lee, C. Cho, Y. Ryuh: Design and control of 3-DOF robotic fish 'ICHTHUS V5', *Lect. Not. Comp. Sci.* **8103**, 310–319 (2013)
- 23.74 K. Low: Modelling and parametric study of modular undulating fin rays for fish robots, *Mech. Mach. Theory* **44**, 615–632 (2009)
- 23.75 A.D. Marchese, C.D. Onal, D. Rus: Autonomous soft robotic fish capable of escape maneuvers using fluidic elastomer actuators, *Soft Robotics* **1**, 75–87 (2014)
- 23.76 Z. Chen, T.I. Um, H. Bart-Smith: Bio-inspired robotic manta ray powered by ionic polymer-metal composite artificial muscles, *Int. J. Smart Nano Mater.* **3**, 296–308 (2012)
- 23.77 H.-J. Kim, S.-H. Song, S.-H. Ahn: A turtle-like swimming robot using a smart soft composite (SSC) structure, *Smart Mater. Struct.* **22**, 014007 (2013)
- 23.78 C.J. Esposito, J.L. Tangorra, B.E. Flammang, G.V. Lauder: A robotic fish caudal fin: Effects of stiffness and motor program on locomotor performance, *J. Exp. Biol.* **215**, 56–67 (2012)
- 23.79 H. Prahlah, R. Pelrine, S. Stanford, J. Marlow, R. Kornbluh: Electroadhesive robots—wall climbing robots enabled by a novel, robust, and electrically controllable adhesion technology, *Proc. IEEE Int. Conf. Robotics Autom. (ICRA)* (2008) pp. 3028–3033
- 23.80 P. Birkmeyer, A.G. Gillies, R.S. Fearing: CLASH: Climbing vertical loose cloth, *Proc. IEEE/RSJ Int. Conf. Intell. Robots Syst. (IROS)* (2011) pp. 5087–5093
- 23.81 K. Streitlien, G.S. Triantafyllou, M.S. Triantafyllou: Efficient foil propulsion through vortex control, *AIAA J.* **34**, 2315–2319 (1996)
- 23.82 H. Morikawa, S. Nakao, S.-I. Kobayashi: Experimental study on oscillating wing for propulsor with bending mechanism modeled on caudal muscle-skeletal structure of tuna, *Jap. Soc. Mech. Eng. C* **44**, 1117–1124 (2001)
- 23.83 R. Fan, J. Yu, L. Wang, G. Xie, Y. Fang, Y. Hu: Optimized design and implementation of biomimetic robotic dolphin, *IEEE Int. Conf. Robotics Biomimet. (ROBIO)* (2005) pp. 484–489
- 23.84 T. Salumäe, M. Kruusmaa: A flexible fin with bio-inspired stiffness profile and geometry, *J. Bionic Eng.* **8**, 418–428 (2011)
- 23.85 P.V. y Alvarado, K. Youcef-Toumi: Design of machines with compliant bodies for biomimetic locomotion in liquid environments, *J. Dyn. Syst. Meas. Contr.* **128**, 3–13 (2006)
- 23.86 U. Scarfogliero, C. Stefanini, P. Dario: Design and development of the long-jumping, *Proc. IEEE Int. Conf. Robotics Autom. (ICRA)* (2007) pp. 467–472
- 23.87 M. Kovac, M. Fuchs, A. Guignard, J.-C. Zufferey, D. Floreano: A miniature 7g jumping robot, *Proc. IEEE Int. Conf. Robotics Autom. (ICRA)* (2008) pp. 373–378
- 23.88 Y.-J. Park, T.M. Huh, D. Park, K.-J. Cho: Design of a variable-stiffness flapping mechanism for maximizing the thrust of a bio-inspired underwater robot, *Bioinsp. Biomimet.* **9**, 036002 (2014)
- 23.89 W.-S. Chu, K.-T. Lee, S.-H. Song, M.-W. Han, J.-Y. Lee, H.-S. Kim, M.S. Kim, Y.J. Park, K.J. Cho, S.H. Anh: Review of biomimetic underwater robots using smart actuators, *Int. J. Prec. Eng. Manuf.* **13**, 1281–1292 (2012)
- 23.90 Z. Wang, G. Hang, Y. Wang, J. Li, W. Du: Embedded SMA wire actuated biomimetic fin: A module for biomimetic underwater propulsion, *Smart Mater. Struct.* **17**, 025039 (2008)
- 23.91 G.V. Lauder, J. Lim, R. Shelton, C. Witt, E. Anderson, J.L. Tangorra: Robotic models for studying undulatory locomotion in fishes, *Mar. Technol. Soc. J.* **45**, 41–55 (2011)
- 23.92 F. Li, G. Bonsignori, U. Scarfogliero, D. Chen, C. Stefanini, W. Liu, P. Dario, F. Xin: Jumping mini-robot with bio-inspired legs, *IEEE Int. Conf. Robotics Biomimet. (ROBIO)* (2009) pp. 933–938
- 23.93 B.G.A. Lambrecht, A.D. Horchler, R.D. Quinn: A small, insect-inspired robot that runs and jumps, *Proc. IEEE Int. Conf. Robotics Autom. (ICRA)* (2005) pp. 1240–1245
- 23.94 J. Zhao, J. Xu, B. Gao, N. Xi, F.J. CINTRÓN, M.W. Mutka, X. Li: MSU Jumper: A single-motor-actuated miniature steerable jumping robot, *IEEE Trans. Robotics* **29**, 602–614 (2013)
- 23.95 J. Zhao, W. Yan, N. Xi, M.W. Mutka, L. Xiao: A miniature 25 grams running and jumping robot, *Proc. IEEE Int. Conf. Robotics Autom. (ICRA)* (2014)
- 23.96 R. Armour, K. Paskins, A. Bowyer, J. Vincent, W. Megill: Jumping robots: A biomimetic solution to locomotion across rough terrain, *Bioinsp. Biomimet.* **2**, S65–S82 (2007)

- 23.97 M. Noh, S.-W. Kim, S. An, J.-S. Koh, K.-J. Cho: Flea-inspired catapult mechanism for miniature jumping robots, *IEEE Trans. Robotics* **28**, 1007–1018 (2012)
- 23.98 J.-S. Koh, S.-P. Jung, M. Noh, S.-W. Kim, K.-J. Cho: Flea inspired catapult mechanism with active energy storage and release for small scale jumping robot, *Proc. IEEE Int. Conf. Robotics Autom. (ICRA)* (2013) pp. 26–31
- 23.99 J.-S. Koh, S.-P. Jung, R.J. Wood, K.-J. Cho: A jumping robotic insect based on a torque reversal catapult mechanism, *Proc. IEEE/RSJ Int. Conf. Intell. Robots Syst. (IROS)* (2013) pp. 3796–3801
- 23.100 A. Yamada, M. Watari, H. Mochiyama, H. Fujimoto: An asymmetric robotic catapult based on the closed elastica for jumping robot, *Proc. IEEE Int. Conf. Robotics Autom. (ICRA)* (2008) pp. 232–237
- 23.101 A.P. Gerratt, S. Bergbreiter: Incorporating compliant elastomers for jumping locomotion in micro-robots, *Smart Mater. Struct.* **22**, 014010 (2013)
- 23.102 R. Niiyama, A. Nagakubo, Y. Kuniyoshi: Mowgli: A bipedal jumping and landing robot with an artificial musculoskeletal system, *Proc. IEEE Int. Conf. Robotics Autom. (ICRA)* (2007) pp. 2546–2551
- 23.103 E.W. Hawkes, E.V. Eason, A.T. Asbeck, M.R. Cutkosky: The gecko's toe: Scaling directional adhesives for climbing applications, *IEEE/ASME Trans. Mechatron.* **18**, 518–526 (2013)
- 23.104 E.W. Hawkes, D.L. Christensen, E.V. Eason, M.A. Estrada, M. Heverly, E. Hilgemann, J. Hao, M.T. Pope, A. Parness, M.R. Cutkosky: Dynamic surface grasping with directional adhesion, *Proc. IEEE/RSJ Int. Conf. Intell. Robots Syst. (IROS)* (2013) pp. 5487–5493
- 23.105 A.L. Desbiens, A.T. Asbeck, M.R. Cutkosky: Landing, perching and taking off from vertical surfaces, *Int. J. Robotics Res.* **30**, 355–370 (2011)
- 23.106 A. Parness, M. Frost, N. Thatte, J.P. King, K. Witkoe, M. Nevarez, M. Garrett, H. Aghazarian, B. Kennedy: Gravity-independent rock-climbing robot and a sample acquisition tool with microspine grippers, *J. Field Robotics* **30**, 897–915 (2013)
- 23.107 B.A. Trimmer, A.E. Takesian, B.M. Sweet, C.B. Rogers, D.C. Hake, D.J. Rogers: Caterpillar locomotion: A new model for soft-bodied climbing and burrowing robots, *7th Int. Symp. Technol. Mine Problem* (2006) pp. 1–10
- 23.108 G.-P. Jung, J.-S. Koh, K.-J. Cho: Underactuated adaptive gripper using flexural buckling, *IEEE Trans. Robotics* **29**(6), 1396 (2013)
- 23.109 M. Calisti, M. Giorelli, G. Levy, B. Mazzolai, B. Hochner, C. Laschi, P. Dario: An octopus-bio-inspired solution to movement and manipulation for soft robots, *Bioinsp. Biomimet.* **6**, 036002 (2011)
- 23.110 S.-W. Kim, J.-S. Koh, J.-G. Lee, J. Ryu, M. Cho, K.-J. Cho: Flytrap-inspired robot using structurally integrated actuation based on bistability and a developable surface, *Bioinsp. Biomimet.* **9**, 036004 (2014)
- 23.111 C.E. Doyle, J.J. Bird, T.A. Isom, J.C. Kallman, D.F. Bareiss, D.J. Dunlop, R.J. King, J.J. Abbott, M.A. Minor: An avian-inspired passive mechanism for quadrotor perching, *IEEE/ASME Trans. Mechatron.* **18**, 506–517 (2013)
- 23.112 M. Kovač, J. Germann, C. Hürzeler, R.Y. Siegwart, D. Floreano: A perching mechanism for micro aerial vehicles, *J. Micro-Nano Mechatron.* **5**, 77–91 (2009)
- 23.113 R. Merz, F. Prinz, K. Ramaswami, M. Terk, L. Weiss: Shape deposition manufacturing, *Proc. Solid Freeform Fabric. Symp.*, University of Texas at Austin (1994) pp. 1–8
- 23.114 S.A. Bailey, J.G. Cham, M.R. Cutkosky, R.J. Full: Biomimetic robotic mechanisms via shape deposition manufacturing, *Robotics Res. Int. Symp.* (2000) pp. 403–410
- 23.115 X. Li, A. Golnas, F.B. Prinz: Shape deposition manufacturing of smart metallic structures with embedded sensors, *SPIE Proc. 7th Annu. Int. Symp. Smart Struct. Mater. (International Society for Optics and Photonics, Bellingham 2000)* pp. 160–171
- 23.116 K.G. Marra, J.W. Szem, P.N. Kumta, P.A. DiMilla, L.E. Weiss: In vitro analysis of biodegradable polymer blend/hydroxyapatite composites for bone tissue engineering, *J. Biomed. Mater. Res.* **47**, 324–335 (1999)
- 23.117 J.G. Cham, S.A. Bailey, J.E. Clark, R.J. Full, M.R. Cutkosky: Fast and robust: Hexapedal robots via shape deposition manufacturing, *Int. J. Robotics Res.* **21**, 869–882 (2002)
- 23.118 A.M. Dollar, R.D. Howe: A robust compliant grasper via shape deposition manufacturing, *IEEE/ASME Trans. Mechatron.* **11**, 154–161 (2006)
- 23.119 M. Binnard, M.R. Cutkosky: Design by composition for layered manufacturing, *J. Mech. Des.* **122**, 91–101 (2000)
- 23.120 Y.-L. Park, K. Chau, R.J. Black, M.R. Cutkosky: Force sensing robot fingers using embedded fiber Bragg grating sensors and shape deposition manufacturing, *IEEE Int. Conf. Robotics Autom. (ICRA)* (2007) pp. 1510–1516
- 23.121 D. Shin, I. Sardellitti, Y.-L. Park, O. Khatib, M. Cutkosky: Design and control of a bio-inspired human-friendly robot, *Int. J. Robotics Res.* **29**, 571–584 (2010)
- 23.122 R.S. Fearing, K.H. Chiang, M.H. Dickinson, D.L. Pick, M. Sitti, J. Yan: Wing transmission for a micromechanical flying insect, *Proc. IEEE Int. Conf. Robotics Autom. (ICRA)*, Vol. 2 (2000) pp. 1509–1516
- 23.123 J. Yan, R.J. Wood, S. Avadhanula, M. Sitti, R.S. Fearing: Towards flapping wing control for a micromechanical flying insect, *Proc. IEEE Int. Conf. Robotics Autom. (ICRA)* (2001) pp. 3901–3908
- 23.124 R.J. Wood, S. Avadhanula, M. Menon, R.S. Fearing: Microrobotics using composite materials: The micromechanical flying insect thorax, *Proc. IEEE Int. Conf. Robotics Autom. (ICRA)*, Vol. 2 (2003) pp. 1842–1849

- 23.125 K.Y. Ma, P. Chirarattananon, S.B. Fuller, R.J. Wood: Controlled flight of a biologically inspired, insect-scale robot, *Science* **340**, 603–607 (2013)
- 23.126 J. Whitney, P. Sreetharan, K. Ma, R. Wood: Pop-up book MEMS, *J. Micromech. Microeng.* **21**, 115021 (2011)
- 23.127 P.S. Sreetharan, J.P. Whitney, M.D. Strauss, R.J. Wood: Monolithic fabrication of millimeter-scale machines, *J. Micromech. Microeng.* **22**, 055027 (2012)
- 23.128 C. Majidi: Soft robotics: A perspective – Current trends and prospects for the future, *Soft Robotics* **1**, 5–11 (2013)
- 23.129 Y. Xia, G.M. Whitesides: Soft lithography, *Annu. Rev. Mater. Sci.* **28**, 153–184 (1998)
- 23.130 F. Ilievski, A.D. Mazzeo, R.F. Shepherd, X. Chen, G.M. Whitesides: Soft robotics for chemists, *Angew. Chem.* **123**, 1930–1935 (2011)
- 23.131 R.F. Shepherd, F. Ilievski, W. Choi, S.A. Morin, A.A. Stokes, A.D. Mazzeo, X. Chen, M. Wang, G.M. Whitesides: Multigait soft robot, *Proc. Natl. Acad. Sci.* **108**, 20400–20403 (2011)
- 23.132 B.C.-M. Chang, J. Berring, M. Venkataram, C. Menon, M. Parameswaran: Bending fluidic actuator for smart structures, *Smart Mater. Struct.* **20**, 035012 (2011)
- 23.133 B. Chang, A. Chew, N. Naghshineh, C. Menon: A spatial bending fluidic actuator: Fabrication and quasi-static characteristics, *Smart Mater. Struct.* **21**, 045008 (2012)
- 23.134 B. Finio, R. Shepherd, H. Lipson: Air-Powered Soft Robots for K–12 Classrooms, *IEEE Proc. Integr. STEM Edu. Conf. (ISEC)* (2013) pp. 1–6
- 23.135 S.A. Morin, R.F. Shepherd, S.W. Kwok, A.A. Stokes, A. Nemiroski, G.M. Whitesides: Camouflage and display for soft machines, *Science* **337**, 828–832 (2012)
- 23.136 R.V. Martinez, J.L. Branch, C.R. Fish, L. Jin, R.F. Shepherd, R. Nunes, Z. Suo, G.M. Whitesides: Robotic tentacles with three-dimensional mobility based on flexible elastomers, *Adv. Mater.* **25**, 205–212 (2013)
- 23.137 R.V. Martinez, C.R. Fish, X. Chen, G.M. Whitesides: Elastomeric origami: Programmable paper-elastomer composites as pneumatic actuators, *Adv. Funct. Mater.* **22**, 1376–1384 (2012)
- 23.138 S.W. Kwok, S.A. Morin, B. Mosadegh, J.H. So, R.F. Shepherd, R.V. Martinez, B. Smith, F.C. Simeone, A.A. Stokes, G.M. Whitesides: Magnetic assembly of soft robots with hard components, *Adv. Funct. Mater.* **24**, 2180–2187 (2013)
- 23.139 B. Mosadegh, P. Polygerinos, C. Keplinger, S. Wennstedt, R.F. Shepherd, U. Gupta, J. Shim, K. Bertoldi, C.J. Walsh, G.M. Whitesides: Pneumatic networks for soft robotics that actuate rapidly, *Adv. Funct. Mater.* **24**, 2163–2170 (2013)
- 23.140 M. Cianchetti, A. Arienti, M. Follador, B. Mazzolai, P. Dario, C. Laschi: Design concept and validation of a robotic arm inspired by the octopus, *Mater. Sci. Eng. C* **31**, 1230–1239 (2011)
- 23.141 T. Umedachi, V. Vikas, B.A. Trimmer: Highly deformable 3-D printed soft robot generating inching and crawling locomotions with variable friction legs, *Proc. IEEE/RSJ Int. Conf. Intell. Robots Syst. (IROS)* (2013) pp. 4590–4595